Respiratory infection promotes T cell infiltration and Aβ deposition in APP/PS1 mice

Róisín M. McManus,*,† Sarah C. Higgins,† Kingston H. G. Mills,†,[1] and Marina A. Lynch*,[1]

*Trinity College Institute of Neuroscience, Trinity Biomedical Sciences Institute, Trinity College Dublin, Dublin 2, Ireland and †School of Biochemistry and Immunology, Trinity Biomedical Sciences Institute, Trinity College Dublin, Dublin 2, Ireland.

[1]K.H.G.M. and M.A.L. contributed equally to this work.

Address correspondence and reprint requests to Róisín M. McManus, Trinity College Institute of Neuroscience, Trinity Biomedical Sciences Institute, Trinity College Dublin, Dublin 2, Ireland.

E-mail address: mcmanur@tcd.ie

Phone: +353 1 8968473

Fax: +353 1 8963183

Abstract

Alzheimer's disease (AD) is a progressive neurodegenerative disease characterized by deposits of amyloid-β and neurofibrillary tangles. It has been suggested that inflammatory changes are associated with disease; however, it has not been established if these are a consequence of ongoing neurodegeneration or whether inflammation itself contributes to disease pathogenesis. Recent studies suggest that exposure to infection can accelerate cognitive decline in AD patients, and pathogens have been detected in the AD brain. However, the influence of infection on neuroinflammation and pathology remains poorly understood. In this study, we examined the effect of a peripheral infection on AD pathology in APP/PS1 mice. We found that, 8 weeks after infection with the Gram negative respiratory pathogen *Bordetella pertussis*, there was significant infiltration of IFNγ- and IL-17-producing T cells and NKT cells in older APP/PS1 mice. This was accompanied by increased glial activation and amyloid β deposition. The data suggest that infection is a critical factor in the progression of AD, emphasising the importance of early diagnosis and treatment of infections in elderly individuals.

Key words: Alzheimer's disease, infection, T cell, microglia, amyloid β, neuroinflammation

1. Introduction

Alzheimer's disease (AD) is the most common neurodegenerative disease and accounts for more than two-thirds of all dementia cases. It is a progressive disease characterized by neurofibrillary tangles and deposits of amyloid-β (Aβ). These protein deposits are associated with dystrophic neurons, reactive astrocytes, and activated microglia. It is estimated that AD affects about 20 million persons worldwide, and this figure is expected to reach more than 100 million by 2050 (Williams, 2009).

Although the aetiology of AD is unknown, there is evidence to suggest that inflammatory responses play a role in its pathogenesis (Mattson, 2004,Weiner and Frenkel, 2006). Pro-inflammatory cytokines and chemokines are increased in AD brain tissue (Akiyama, et al., 2000,Streit, et al., 2001). Activated microglia have been found in the brain of AD patients with dementia or patients with mild cognitive impairment (Cagnin, et al., 2001,Okello, et al., 2009) and these cells secrete pro-inflammatory cytokines, such as interleukin (IL)-1β and tumor necrosis factor (TNF)α. These cytokines promote expression and activity of β-secretases and γ-secretases (Liao, et al., 2004,Sastre, et al., 2008), and therefore microglial activation may contribute to deposition of Aβ and progression of AD (Glass, et al., 2010). Activated microglia exhibit increased expression of major histocompatibility complex (MHC) class II, CD80 and CD86 (Aloisi, et al., 2000,McQuillan, et al., 2010) and, in AD, there is increased MHC class II expression on microglia associated with Aβ plaques (McGeer, et al., 1987), indicating enhanced antigen presenting cell (APC) function. Indeed, it is well established that microglia act as APC for T cells (Aloisi, et al., 2000,McQuillan, et al., 2010,Murphy, et al., 2010). Interestingly, there have been a number of reports demonstrating the presence of T cells in the brain of AD patients (Hartwig, 1995,McGeer, et al., 1989,Parachikova, et al., 2007,Pirttila, et al., 1992,Togo, et al., 2002,Town, et al., 2005), since the original observation 25 years ago (Rogers, et al., 1988). Furthermore, inflammatory IFNγ-secreting Th1 cells and IL-17-secreting

Th17 cells have been shown to infiltrate the brain of older APP/PS1 mice (Browne, et al., 2013).

Although the environmental factors that precipitate the neurological changes associated with the development of AD are unclear, it has been suggested that infectious agents may be involved. Herpes simplex virus type 1 (HSV1) and *Chlamydia pneumonia*, as well as antibodies against these pathogens, have been found in the post-mortem brains (Hammond, et al., 2010) or intrathecal samples (Wozniak, et al., 2005) of AD patients. Indeed HSV1 infection has been suggested to be a risk factor in carriers of the gene for apolipoprotein E type 4 (APO-E4) (Honjo, et al., 2009,Itzhaki, et al., 2004), whereas viral load is related to ApoE expression especially ApoE4 (Burgos, et al., 2006). Spirochetes, particularly *Borrelia burgdorferi* and oral *Treponema* (Honjo, et al., 2009) and cytomegalovirus (Lurain, et al., 2013) have also been implicated as playing a role in the pathogenesis of AD. Furthermore, a number of studies have shown that infections can accelerate cognitive decline in AD patients (Holmes, et al., 2009,Holmes, et al., 2003), but there is little understanding of the mechanisms that underlie this effect. Animal studies have revealed that intranasal inoculation of mice with *C. pneumoniae* induced AD-like changes in brain, with evidence of deposits of fibrillar Aβ associated with reactive glia in several brain areas including the hippocampus (Little, et al., 2004). Similarly, peripheral challenge with the Toll-like receptor (TLR) agonists, lipopolysaccharide (LPS), or polyriboinosinic-polyribocytidilic acid (PolyI:C) induced amyloid pathology in some (Krstic, et al., 2012,Sheng, et al., 2003), but not all (Kitazawa, et al., 2005), animal models of AD. However it has been observed that activation of the immune system may also prove beneficial in AD, as administration of a vaccine (Butovsky, et al., 2006,Olkhanud, et al., 2012,Schenk, et al., 1999) or TLR agonist (Michaud, et al., 2013) was effective in clearing Aβ load and, in some cases, preventing cognitive decline in mice. It has also been suggested that bone-marrow

derived dendritic cells (Butovsky, et al., 2007) and bone marrow derived microglia (Simard, et al., 2006) have an important role in plaque clearance.

In this study, we examined the influence of a peripheral infection with a respiratory pathogen *Bordetella pertussis* on AD-like pathology in transgenic mice that overexpress amyloid precursor protein (APP) with the Swedish double mutation and exon-9 deleted presenilin 1 (PS1; APP/PS1). *B. pertussis* is a Gram-negative bacteria that causes whooping cough, a persistent and sometimes fatal disease in young children, but also an emerging problem in adults and older people. Recent studies have shown that the prevalence of *B. pertussis* infection is high in adults and increasing at a significant rate, especially in individuals more than 65 years of age (Weston, et al., 2012)**.** Our objective was to establish whether older APP/PS1 mice were more susceptible to the effects of peripheral infection than younger animals. Specifically, we asked whether any change in AD-like pathology was accompanied by infiltration of inflammatory T cells, which we have previously shown to drive neuroinflammation and pathology.

2. Methods

2.1 Animals

APP/PS1 mice and wild-type (WT) littermates (4 and 10 months of age) were obtained from the Jackson Laboratory (USA) and bred in a specific pathogen-free unit in the Bioresources Unit, Trinity College Dublin. All mice were maintained in controlled conditions (temperature, 22°C–23°C; 12-hour light-dark cycle; food and water *ad libitum*) under veterinary supervision, and experimentation was carried out under a license granted by the Minister for Health and Children (Ireland) and with the appropriate ethical approval.

2.2 B. pertussis respiratory challenge

Respiratory infection of male and female, WT and APP/PS1 mice was induced by aerosol challenge as described elsewhere (McGuirk, et al., 1998). *B. pertussis* Wellcome 28 was streaked onto Bordet-Gengou agar plates and grown at 37°C for 4 days, and bacteria were transferred to Stainer-Scholte liquid medium for 24 hours at 37°C. Bacteria were resuspended at 1.7 x 10^{10} colony forming units (CFU)/mL in physiological saline containing 1% casein, and aerosol challenge was administered over a period of 15 minutes using a nebulizer; this was followed by a rest period of 10 minutes before returning the mice to their cages. Infection with the pathogen was confirmed by performing CFU counts on the lungs of mice 3 hours and 21 days postinfection. The lungs were aseptically removed and homogenized in 1 mL of sterile 1% casein on ice. Undiluted and serially diluted lung homogenate was spread onto Bordet-Gengou agar plates, and the CFU was established after 5 days of incubation at 37°C.

2.3 Isolation and flow cytometry analysis on mononuclear cells from CNS tissue

APP/PS1 mice and nontransgenic littermates were anaesthetized with sodium pentobarbital (40 µL) and perfused intracardially with sterile ice-cold phosphate-buffered saline (PBS) solution (20 mL). The brain was removed and placed in RPMI solution supplemented with 1% penicillin-streptomycin, 1% L-glutamine and 10% fetal bovine serum (FBS; Sigma-Aldrich). A single cell suspension was prepared by passing the tissue through a sterile, 70-µm-pore nylon mesh filter, washed with complete RPMI solution and centrifuged at 1,200 rpm for 5 minutes. The supernatant was removed and the remaining pellet was resuspended in complete RPMI (2 mL) containing collagenase D (1 mg/mL, Roche, Ireland) and DNAse I (10 µg/mL, Sigma-Aldrich), and incubated for 1 hour at 37^{o}C with agitation. Cells were washed in complete RPMI and centrifuged at 1,200 rpm for 5 minutes. The supernatants were discarded and cells were resuspended in 1.088 g/mL Percoll (9 mL; Sigma-Aldrich). This solution was underlayed with 1.122g/mL Percoll (5 mL) and overlayed with 1.072 g/mL Percoll (9 mL), 1.030g/mL Percoll (9 mL) and PBS (9 mL). Samples were centrifuged

at 1,250 x g for 45 minutes. Mononuclear cells were removed from the 1.088:1.072 and 1.072:1.030-g/mL interfaces, washed twice in complete RPMI, and counted.

Samples which were intended for intracellular staining to identify T cell subsets were centrifuged at 1,200 rpm for 5 minutes and cells were incubated in the presence of phorbol myristate acetate (PMA; 10 ng/mL; Sigma-Aldrich), ionomycin (1 μg/mL; Sigma-Aldrich), and brefeldin A (BFA; 5 μg/mL; Sigma-Aldrich) for 5 hours, centrifuged at 1,200 rpm for 5 minutes, resuspended in 50 μL PBS with 1:1000 LIVE/DEAD® Fixable Aqua Dead Cell Stain kit (Life Technologies) for 20 minutes, washed, and resuspended in 50 μL fluorescence activated cell sorting (FACS) buffer containing CD16/CD32 FcγRIII (1:100) for 10 minutes to block low-affinity IgG receptors and thus prevent nonspecific binding of antibodies. Cells were prepared for intracellular staining using a cell permeabilisation kit (Dako, Denmark). For surface labelling, cells were incubated in 50 μL per sample FACS buffer, containing the appropriate antibodies, for 15 minutes at room temperature (RT) at a 1:100 dilution. These antibodies were CD45 (eFlour® 605NC, eBioscience), CD3 (APC, eBioscience), CD4 (A700, eBioscience), CD8 (APC-eFluor® 780, eBioscience) and NK1.1 (PerCPCy5.5, eBioscience). Samples were fixed using IntraStain Reagent A (50 μL/sample; Dako, Denmark) for 15 minutes at RT, washed twice with FACS buffer, centrifuged at 1,200 rpm for 5 minutes and permeabilized with IntraStain Reagent B (50 μL/sample; Dako, Denmark) including intracellular antibodies (IFNγ; PeCy7, eBioscience and IL-17A; V450, BD Biosciences at 1:50 dilution) for 15 minutes at RT in the dark. The cells were washed twice in FACS buffer and centrifuged at 1,200 rpm for 5 minutes. The appropriate compensation controls and fluorescence minus one (FMO) controls were also prepared during this time.

In separate FACS tubes, mononuclear cells which were not stimulated with PMA, ionomycin, or BFA were surface- stained only to identify macrophage and microglial cells.

These samples were blocked for 10 minutes with CD16/CD32 FcγRIII (1:100) to block nonspecific low-affinity IgG receptors which are expressed on a range of cell types including APCs. Samples were incubated with the cell surface antibodies for 15 minutes, which included CD45 (eFluor® 605NC, eBioscience), CD11b (APC-eFluor® 780, eBioscience), CD80 (V450, BD Bioscience), and CD68 (Alexa Fluor® 488, AbD Serotec) at a 1:100 dilution, washed twice in FACS buffer and centrifuged at 1,200 rpm for 5 minutes. Propidium iodide (PI; Sigma-Aldrich) was added (1:100) immediately before reading the samples and was used as a live/dead stain. The appropriate compensation controls and FMO controls were also prepared.

Flow cytometric analysis was performed on an LSR Fortessa, and data acquired using Summit software (Dako, Denmark). The results were analysed using FlowJo software (Tree Star, USA). All T cells were identified as being negative for LIVE/DEAD® Fixable Aqua Dead Cell Stain, $CD45^+$, and $CD3^+$. T helper cells were identified as $CD45^+CD3^+CD4^+$ cells, whereas cytotoxic T cells were identified as $CD45^+CD3^+CD8^+$ cells. NKT cells were identified as $CD45^+CD3^+NK1.1^+$. Microglia were identified as being $CD11b^+CD45^{low}$ cells, and macrophages were identified as $CD11b^+CD45^{high}$ cells, which is consistent with previous reports (Becher and Antel, 1996,Sedgwick, et al., 1991); although a $CD11b^+CD45^{low/medium}$ population of microglial cells has been observed (Dick, et al., 1997), we found CD45 expression to be either high or low on the $CD11b^+$ cells.

2.4 Preparation of tissue

After 56 days mice were anaesthetized with sodium pentobarbital (40 µl; Euthatal, Merial Animal Health, UK) and perfused intracardially with ice-cold PBS (20 mL). The brains were rapidly removed and hemisected. A sagittal section of the brain was taken for immunohistochemical analysis, placed onto cork discs, covered with optimum cooling

temperature compound (OCT; Sakura Tissue-Tek, Netherlands), snap-frozen in isopropanol on dry ice and stored at -80°C. Cortical tissue was taken and snap-frozen in liquid nitrogen and stored at -80°C for analysis of Aβ, and cortical tissue was also snap-frozen for later mRNA analysis. The remaining brain tissue was used to prepare mononuclear cells for flow-cytometric analysis as described above.

2.5 Detection of Aβ

Detergent-soluble and insoluble Aβ was assessed using MSD® 96-well multi-spot 4G8 Aβ triple ultra-sensitive assay kits according to the manufacturer's instructions (Meso Scale Discovery, US). Snap-frozen cortical tissue was homogenized in 50mmol/L NaCl (pH10) with 1% sodium dodecyl sulphate (SDS) and centrifuged (15,000 rpm for 40 minutes at 4^{o}C). The supernatant, which was used for analysis of detergent-soluble Aβ, was equalized to 5 mg/mL total protein and stored at -20^{o}C. For analysis of insoluble Aβ, the pellets were incubated in guanidine buffer (200 μL; 5 mol/L guanidine-HCl/50 mmol/L Tris-HCl, pH 8, Sigma-Aldrich) for 4 hours at RT with agitation; this step enables the protein to be solubilized and denatured to give the monomeric form and be assessed relative to the standards that are supplied by the manufacturer as lyophilized peptides. Samples were centrifuged (15,000 rpm for 30 minutes at 4^{o}C) and the supernatant samples were equalized to 0.1 mg/mL with guanidine buffer and stored at -20^{o}C. Standards ($A\beta_{1-38}$, 0-3,000 pg/mL; $A\beta_{1-40}$, 0-10,000 pg/mL; $A\beta_{1-42}$, 0-3,000 pg/mL) and samples were added to the 96-well plates, incubated (2 hours, RT), washed, and read in a Sector Imager plate reader (Meso Scale Discovery, US) immediately after addition of the MSD read buffer. Aβ concentrations were calculated with reference to the standard curves and expressed as picograms per milliliter.

2.6 Immunohistochemistry

Tissue was allowed to equilibrate to -20^{o}C for 2 hours. Sagittal sections (10-µm thick) were prepared for later staining with Congo red to assess Aβ plaque deposition using a cryostat (Leica, Meyer, UK), mounted on gelatine-coated glass slides (Fluka, Switzerland), allowed to dry for 20 minutes, and stored at -20°C for later immunohistochemical analysis. Sections, which were allowed to equilibrate to room temperature for 30 minutes, were fixed in ice-cold methanol for 5 minutes, washed in PBS, and incubated at RT for 20 minutes in saturated NaCl (200 mL; 80% ethanol in dH_2O) supplemented with NaOH (2 mL; 1 mol/L). Sections were incubated in filtered Congo red solution (200 mL; 0.2% Congo red dye in saturated NaCl solution with 2mL NaOH; 1 mol/L) for 30 minutes and rinsed in dH_2O. The slides were incubated in methyl green solution (1% in dH_2O) for 30 seconds, washed, and dehydrated by dipping in 95% and then 100% ethanol. Sections were dried, incubated in 100% xylene (3 x 5 min) and mounted using dibutyl phthalate in xylene (DPX; RA Lamb, UK). Slides were allowed to dry overnight, stored at RT, and later examined using an Olympus lx51 light microscope (Tokyo, Japan). Micrographs were taken using an Olympus UCMAD3 (Japan) at x10 magnification.

2.7 Real-time polymerase chain reaction

Total RNA was extracted from snap-frozen cortical tissue using the NucleoSpin® RNAII isolation kit (Macherey-Nagel, Germany). Total RNA concentrations were determined using spectrophotometry, samples were equalized and cDNA synthesis was performed on 1 µg total RNA using a High Capacity cDNA RT kit (Applied Biosystems, Germany). Real-time polymerase chain reaction (PCR) was performed for the detection of CCL3 (Mm00441258_m1), CXCL10 (Mm00445235_m1), CCL5 (Mm01302428_m1), CD11b (Mm00434455_m1), GFAP (Mm01253033_m1), TNFα (Mm00443258_m1), IL-1β (Mm00434228_m1), and IL-6 (Mm00446190_m1), using Taqman Gene Expression Assays (Applied Biosystems, Germany). Real-time PCR was conducted using an ABI Prism 7300

instrument (Applied Biosystems, Germany). A 25 µL volume was added to each well (2.5 µL of cDNA, 1.25 µL of each primer, 12.5 µL of SensiMix^{TM} II Probe Mastermix (Bioline) and 7.5 µL of nuclease free H_20). 18S ribosomal RNA was the endogenous control (VIC labelled Taqman probe, Applied Biosystems, Germany; Assay ID 4319413E). Gene expression was calculated relative to the endogenous control and to the averaged young WT uninfected control samples giving an RQ value (2^{-DDCt}, where Ct is the threshold cycle).

2.8 Statistical analysis

Statistical analysis was performed using GraphPad Prism or GB-STAT. Data were analysed using 2-way analysis of variance (ANOVA) (to investigate age x infection interactions) or 3-way ANOVA (to determine age x genotype x infection interactions) followed by Bonferroni or Newman-Keuls post-hoc test. Data are expressed as means with standard errors of the mean (SEM) and deemed statistically significant when $p<0.05$.

3. Results

3.1 Infection induced increased T cell infiltration into the brains of APP/PS1 mice

Young (4 months) and older (10 months) WT and APP/PS1 mice were infected with *B. pertussis* by aerosol challenge with live bacteria. Evidence of successful infection was provided by performing CFU counts on lung homogenates removed from groups of mice 3 hours and 21 days after challenge. The mean CFU counts were $\log_{10}$ 4.7 and 3.0 at 3 hours and 21 days, respectively, which is consistent with our previous studies (Dunne, et al., 2010,Ross, et al., 2013). Mice were killed 56 days postinfection, 3 weeks after the pathogen is normally cleared (McGuirk, et al., 1998), and brain tissue was prepared for flow cytometry to assess infiltration of immune cells. The number of $CD3^+CD45^+$ T cells was doubled in brains of 12-month-old

compared with 6-month-old mice, but was significantly greater in older *B. pertussis*-infected APP/PS1 mice when compared with genotype-matched, age-matched or noninfected controls (**$p < 0.01$ vs. older infected WT, $^{++}p < 0.01$ vs. young infected APP/PS1, and $^{\#\#}p < 0.01$ vs. older APP/PS1 control; Fig. 1A). Analysis of the T cell subtypes also showed that infection with *B. pertussis* caused a significant increase in the number of $CD4^+$ and $CD8^+$ T cells in the brain of older APP/PS1 mice (***$p < 0.0001$ and **$p < 0.01$; Fig. 1B, C respectively), and there was an age-related increase in the number of $CD8^+$ T cells in APP/PS1 mice at 12 months (**$p < 0.01$; Fig. 1C). Intracellular cytokine staining revealed that a proportion of the brain-infiltrating $CD4^+$ T cells were $IFN\gamma^+$ with overall significant increase in Th1-type cells in *B. pertussis* infected mice (*$p < 0.05$; Fig. 2A). Interestingly, there was a significant increase in the number of IL-17^+ and $IFN\gamma^+$IL-17^+ $CD4^+$ T cells in *B. pertussis*-infected mice ($^{\#}p < 0.05$ and $^{\#\#}p < 0.01$ vs. uninfected controls; Fig. 2B and C). Similar results were obtained for $CD8^+$ T cells, with an infection induced increase in IFNγ secreting $CD8^+$ T cells, especially in the older APP/PS1 mice (**$p < 0.01$ vs. older infected WT, $^{++}p < 0.01$ vs. young infected APP/PS1, and $^{\#}p < 0.05$ vs. older APP/PS1 control; Fig. 2E). The number of infiltrating IL-17^+ and $IFN\gamma^+$IL-17^+ $CD8^+$ T cells was also enhanced in brains of infected mice (**$p < 0.01$ vs. older infected WT, $^{++}p < 0.01$ vs. young infected APP/PS1, and $^{\#\#}p < 0.01$ vs. older APP/PS1 control; Fig. 2F and G).

There was also a significant increase in the number of $NK1.1^+CD3^+CD45^+$ T cells in the brain of 12-month-old *B. pertussis*-infected APP/PS1 mice (**$p < 0.01$ vs. older infected WT, $^{++}p < 0.01$ vs. young infected APP/PS1, and $^{\#}p < 0.05$ vs. older APP/PS1 control; Fig. 3A) and parallel significant increases in the numbers of these cells, which were $IFN\gamma^+$ (**$p < 0.01$ vs. older infected WT, $^{++}p < 0.01$ vs. young infected APP/PS1, and $^{\#}p < 0.05$ vs. older APP/PS1 control; Fig. 3B) and IL-17^+ (**$p < 0.01$ vs. older infected WT, $^{++}p < 0.01$ vs. young infected APP/PS1, and $^{\#\#}p < 0.01$ vs. older APP/PS1 control; Fig. 3C).

We next examined expression of chemokines, which are chemoattractant for T cells, using RNA extracted from snap-frozen cortical tissue. CCL3 was significantly increased in APP/PS1 mice even at 6 months, and expression increased further with age, particularly in *B. pertussis*-infected APP/PS1 mice (**$p < 0.01$ vs. older infected WT, $^{++}p < 0.01$ vs. young infected APP/PS1, and $^{\#\#}p < 0.01$ vs. older APP/PS1 control; Fig. 4A). CXCL10 was significantly increased in older APP/PS1 mice (**$p < 0.01$ vs. older WT and $^{++}p < 0.01$ vs. young APP/PS1; Fig. 4B) and CCL5 expression was significantly increased with infection, with an age x genotype interaction also evident (*$p < 0.05$ and **$p < 0.01$ respectively; Fig. 4C).

3.2 Increased microglial and macrophage activation in previously infected APP/PS1

Having demonstrated that peripheral infection promoted Th1 and Th17 infiltration into the brain, we assessed the effect of *B. pertussis* infection on microglia and astrocytes, the resident immune cells of the CNS. Expression of CD11b mRNA, which is a marker of microglial activation, and GFAP mRNA, which is a marker of astroglial activation, was increased in the cortex of 12-month-old APP/PS1 mice as previously reported (Gallagher, et al., 2012,Gallagher, et al., 2013), and infection with *B. pertussis* significantly increased expression of both markers (**$p < 0.01$ vs. older infected WT, $^{++}p < 0.01$ vs. young infected APP/PS1, $^{\#}p < 0.05$ and $^{\#\#}p < 0.01$ vs. older APP/PS1 control; Fig. 5A and B). In addition, the number of $CD11b^{+}CD45^{low}$ microglia expressing CD68 was increased in tissue prepared from 12-month-old APP/PS1 mice, and this number was significantly enhanced postinfection in the older APP/PS1 (**$p < 0.01$ vs. older infected WT, $^{++}p < 0.01$ vs. young infected APP/PS1, and $^{\#\#}p < 0.01$ vs. older APP/PS1 control; Fig. 6B).

We assessed the expression of CD80 on microglia and macrophages as an indicator of their antigen presenting capability and found that the number of $CD11b^{+}CD45^{low}$ microglia

expressing CD80 was significantly increased in older infected APP/PS1 mice in comparison with older infected WT mice, with an overall genotype effect observed (**$p < 0.01$; Fig. 6A). The number of $CD80^+$ $CD11b^+CD45^{high}$ macrophages was also significantly increased in preparations from older *B. pertussis*-infected APP/PS1 mice (**$p < 0.01$ vs. older infected WT, $^{++}p < 0.01$ vs. young infected APP/PS1 and $^{\#\#}p < 0.01$ vs. older APP/PS1 control; Fig. 7A). Mirroring the changes observed in microglia, infection caused a significant increase in the number of $CD68^+$ macrophages in the older APP/PS1 mice, although infection also increased the number of these cells in younger *B. pertussis*-infected APP/PS1 mice (**$p < 0.01$ vs. infected WT, $^{++}p < 0.01$ vs. young infected APP/PS1, $^{\#}p < 0.05$ and $^{\#\#}p < 0.01$ vs. APP/PS1 uninfected control; Fig. 7B).

Activated microglia and macrophages produce inflammatory cytokines and, consistent with this, we found that expression of TNFα, IL-1β and IL-6 mRNA was significantly increased in cortical tissue prepared from older *B. pertussis*-infected APP/PS1 mice (**$p < 0.01$ vs. older infected WT, $^{++}p < 0.01$ vs. young infected APP/PS1, and $^{\#}p < 0.05$ vs. older APP/PS1 control; Fig. 8A-C); IL-1β mRNA was also significantly increased in the older uninfected APP/PS1 mice (*$p < 0.05$ vs. older WT and $^{++}p < 0.01$ vs. young APP/PS1; Fig. 8B).

3.3 Infection enhances Aβ accumulation in aged APP/PS1 mice

Deposition of Aβ has been reported in APP/PS1 mice as young as 6 months of age (Jankowsky, et al., 2004). Consistent with this, we found Aβ-containing plaques in the hippocampus and the frontal cortex in cryostat sections prepared from 6-month-old mice (Fig. 9). Plaque number was significantly increased with age (***$p < 0.001$ vs. young APP/PS1) and interestingly, the number of Aβ containing plaques was further significantly increased in both the hippocampus and frontal cortex of older mice postinfection with *B. pertussis* ($^{+}p < 0.05$, $^{+++}p < 0.001$ vs. older APP/PS1 control; Fig. 9B and D). Analysis of insoluble $A\beta_{40}$ and $A\beta_{42}$ provided further

evidence of age-related increases, which were exacerbated in *B. pertussis*-infected older APP/PS1 mice (**$p < 0.01$ vs. older infected WT, $^{++}p < 0.01$ vs. young infected APP/PS1, and $^{\#\#}p < 0.01$ vs. older APP/PS1 control; Fig. 10C and D). Although detergent-soluble $A\beta_{40}$ and $A\beta_{42}$ both increased in an age-related manner (**$p < 0.01$ vs. older infected WT and $^{++}p < 0.01$ vs. young infected APP/PS1; Fig. 10A and B), no additional effect of infection was observed. These findings demonstrate that a peripheral infection of older APP/PS1 mice can enhance inflammatory T cell infiltration into the brain, and that this is associated the enhanced Aβ burden.

4. Discussion

The significant new findings of this study are that infection of mice with a common human pathogen can induce lasting changes in the brain of older APP/PS1 mice. Specifically a significant number of Th1 and Th17 cells were identified in the brains of 12 month-old APP/PS1 mice, after the resolution of respiratory infection, and this was accompanied by increases in glial activation and Aβ accumulation. These findings suggest that infection may be a major environmental factor in the progression of AD-like pathology.

We report that there was a marked infiltration of T cells, NKT cells and macrophages into the brain of older *B. pertussis*-infected APP/PS1 mice. $CD4^+$ T cells and $CD8^+$ T cells were detected in the brains of both infected and uninfected, 6- and 12-month-old, WT, and APP/PS1 mice but the cell number was markedly enhanced in older *B. pertussis*-infected APP/PS1 mice. Although clearance of *B. pertussis* infection in mice typically occurs in 35 days (McGuirk, et al., 1998), these changes were observed 56 days after infection indicating an age- and genotype-related co-morbidity. The brain-infiltrating T cells were predominantly $IFN\gamma^+$, although infection also triggered infiltration of IL-17^+ T cells into the brains of mice which

were exposed to *B. pertussis*. IFNγ is a potent activator of microglia (Benveniste, et al., 2004,Downer, et al., 2009), and transfer of IFNγ$^+$ T cells to APP/PS1 mice promotes microglial activation and increases plaque burden (Browne, et al., 2013). In vitro, Aβ-specific Th1 cells induce microglial activation, increasing expression of cell surface markers of activation and inducing release of inflammatory cytokines (McQuillan, et al., 2010). Although IL-17$^+$ T cells play a pivotal role in disease pathogenesis in EAE (Mills, 2008), their role in AD is less clear though it has been reported that there is a skewing of T cells in AD to a Th17 phenotype (Saresella, et al., 2011). The present data demonstrate the presence of IL-17$^+$ T cells in the brain, particularly in older *B. pertussis*-infected APP/PS1 mice. Like Aβ-specific Th1 cells, Th17 cells induce microglial activation *in vitro* (McQuillan, et al., 2010) and therefore it seems reasonable to suggest that the presence of both IL-17$^+$ and IFNγ$^+$ T cells combine to trigger the marked increase in activated microglia observed in these mice. Interestingly CD3$^+$ cells have been identified in brain tissue prepared from 18-month-old, but not 6-month-old, APP/PS1 mice (Jimenez, et al., 2008).

An increase in CD11b$^+$CD45^{high}CD80$^+$ and CD11b$^+$CD45^{high}CD68$^+$ macrophages were also observed in brains of *B. pertussis*-infected older APP/PS1 mice. It has been proposed that infiltrating macrophages play a role in phagocytosis of Aβ and therefore exert a protective effect (Town, et al., 2008). However, increased Aβ deposition paralleled macrophage number in the present study, suggesting that their phagocytic potential was limited despite the fact that expression of CD68, a lysosomal marker and proposed indicator of phagocytic function, was increased on macrophages. IFNγ$^+$ NKT cells were also present in the brain of *B. pertussis*-infected older APP/PS1 mice. The role of NKT cells in AD has not been addressed although protective functions for these cells in EAE (Mars, et al., 2008,Mayo, et al., 2012), and in the mutant superoxide dismutase 1 G93A (mSOD1) mouse model of amyotrophic lateral sclerosis (Finkelstein, et al., 2011) have been described. Overall, the significant finding is that infection

drives the infiltration of several IFNγ^+ immune cells, particularly in older APP/PS1 mice, and the evidence indicates that this is associated, ultimately, with increased Aβ pathology.

The first evidence suggesting that T cell infiltration occurred in AD was reported 25 years ago (Rogers, et al., 1988), and since then others have confirmed this observation (Hartwig, 1995,McGeer, et al., 1989,Monsonego, et al., 2003,Parachikova, et al., 2007,Pirttila, et al., 1992,Togo, et al., 2002,Town, et al., 2005). Interestingly these cells have been identified in areas of the brain where amyloid pathology is evident including the hippocampus and limbic regions (Rogers, et al., 1988,Togo, et al., 2002) and have been found in close apposition to activated microglia (Togo, et al., 2002). This suggests the existence of a causal relationship between T cells, microglial activation, and amyloid pathology, which is consistent with the current data demonstrating parallel increases in T cell infiltration, microglial activation, and increased Aβ accumulation. Importantly, our recent work which shows that injection of Aβ-specific Th1 cells into 6- to 7-month-old APP/PS1 mice induced microglial activation and increased Aβ deposition, (Browne, et al., 2013) substantiates this hypothesis.

Infiltration of immune cells may result from the creation of a chemotactic gradient as a consequence of increased expression of chemokines in brain, and here we report that there was an age- and genotype-related increase in expression of CCL3, CXCL10 and CCL5 that was enhanced in *B. pertussis*-infected mice, and all 3 chemokines have established lymphocyte chemotactic properties (Agostini, et al., 2000,Murooka, et al., 2008,Schall, et al., 1993). Interestingly, increased expression of these chemokines has been reported in AD (Tripathy, et al., 2007,Tripathy, et al., 2010,Xia, et al., 2000), whereas increased T cell expression of CCR5 and CXCR2 has also been reported (Liu, et al., 2010,Man, et al., 2007,Reale, et al., 2008). Infiltration of immune cells may also be a consequence of increased blood-brain barrier permeability, which we have observed in aged animals (Blau, et al., 2012) and APP/PS1 mice

(Minogue et al. unpublished), and which is known to occur following *B. pertussis* infection (Linthicum, et al., 1982).

A significant decline in cognitive function has been associated with systemic infection in individuals with AD, and these changes have been linked with persistent increases in circulating inflammatory cytokines (Holmes, et al., 2009,Holmes, et al., 2003). It is also recognized that the risk of developing AD is increased by infection or general ill health, and a particular susceptibility to infection may be conferred by the ApoE e4 allele (Dunn, et al., 2005,Honjo, et al., 2009,Strandberg, et al., 2004,Tilvis, et al., 2004), whereas a protective effect of vaccination has been reported (Tyas, et al., 2001,Verreault, et al., 2001). Interestingly, the incidence of pertussis is increasing in developed countries, probably because of limited efficacy of the current vaccine, and the increase is not only evident in infants but also in adolescents and adults, including those more than 50 years of age (Klein, et al., 2012,McGuiness, et al., 2013).

In the present study, the more profound inflammatory effects induced by infection of older APP/PS1 mice included increased expression of inflammatory cytokines as well as glial activation. These changes were associated with increased concentrations of insoluble $A\beta_{1-40}$ and, albeit to a non-significant extent, $A\beta_{1-42}$, and increased numbers of Congo red-stained Aβ-containing plaques in the frontal cortex and hippocampus. Although the factors that initiate inflammation in AD or models of AD are unknown, the present findings suggest that underlying pathology endows a susceptibility to subsequent infection and enhances pathogenic processes; this is broadly consistent with the finding that infection of 3xTg-AD mice with mouse hepatitis virus induced marked tau pathology postinfection (Sy, et al., 2011). However Stahl et al. (2006) reported that intracerebral infection of Tg2576 mice with the neurotropic Borna disease virus resulted in a decrease in Aβ-containing plaques in hippocampus (Stahl, et al., 2006). Increases in microglial activation and in expression of inflammatory cytokines were observed, prompting the authors to suggest that an inflammatory environment might enhance

clearance of Aβ, which has been supported by some groups (Wilcock, et al., 2011) but not by others (Koenigsknecht-Talboo and Landreth, 2005,Yamamoto, et al., 2007). Indeed it has been shown that an inflammatory environment, such as predominates in AD, inhibits efficient phagocytosis (Koenigsknecht-Talboo and Landreth, 2005), whereas the interaction of microglia with T cells has also been shown to switch microglia from a phagocytic to an APC phenotype (Townsend, et al., 2005). Furthermore, IFNγ has been shown to increase production of Aβ fragments (Liao, et al., 2004,Sastre, et al., 2008), which is important in the present context because of the increased number of $IFN\gamma^+$ cells in the brain of older APP/PS1 mice post infection.

In conclusion, we have demonstrated that infection with a common human pathogen, particularly in older APP/PS1 mice, has profound and persistent effects on inflammatory changes in the brain. The evidence suggests that these changes are driven by infiltration of $IFN\gamma^+$ and IL-17^+ cells and result in exacerbated Aβ pathology. The data point to infection as a significant additional factor in the rapid progression of pathology and highlight the importance of vaccination or treatment of infections in elderly individuals.

Disclosures

Kingston Mills is a co-founder and shareholder in Opsona Therapeutics Ltd and TriMod Therapeutics Ltd, university spin-out companies involved in the development of immunotherapeutics. No other authors have conflicts of interest to declare.

Acknowledgments

This work was supported by grants from Science Foundation Ireland, the Health Research Board, and an Innovation Bursary.

5. References

Agostini, C., Facco, M., Siviero, M., Carollo, D., Galvan, S., Cattelan, A.M., Zambello, R., Trentin, L., Semenzato, G. 2000. CXC chemokines IP-10 and mig expression and direct migration of pulmonary CD8+/CXCR3+ T cells in the lungs of patients with HIV infection and T-cell alveolitis. Am J Respir Crit Care Med 162(4 Pt 1), 1466-73. doi:10.1164/ajrccm.162.4.2003130.

Akiyama, H., Barger, S., Barnum, S., Bradt, B., Bauer, J., Cole, G.M., Cooper, N.R., Eikelenboom, P., Emmerling, M., Fiebich, B.L., Finch, C.E., Frautschy, S., Griffin, W.S., Hampel, H., Hull, M., Landreth, G., Lue, L., Mrak, R., Mackenzie, I.R., McGeer, P.L., O'Banion, M.K., Pachter, J., Pasinetti, G., Plata-Salaman, C., Rogers, J., Rydel, R., Shen, Y., Streit, W., Strohmeyer, R., Tooyoma, I., Van Muiswinkel, F.L., Veerhuis, R., Walker, D., Webster, S., Wegrzyniak, B., Wenk, G., Wyss-Coray, T. 2000. Inflammation and Alzheimer's disease. Neurobiol Aging 21(3), 383-421.

Aloisi, F., Ria, F., Adorini, L. 2000. Regulation of T-cell responses by CNS antigen-presenting cells: different roles for microglia and astrocytes. Immunol Today 21(3), 141-7. doi:S0167569999015121 [pii].

Becher, B., Antel, J.P. 1996. Comparison of phenotypic and functional properties of immediately ex vivo and cultured human adult microglia. Glia 18(1), 1-10. doi:10.1002/(SICI)1098-1136(199609)18:1<1::AID-GLIA1>3.0.CO;2-6.

Benveniste, E.N., Nguyen, V.T., Wesemann, D.R. 2004. Molecular regulation of CD40 gene expression in macrophages and microglia. Brain Behav Immun 18(1), 7-12.

Blau, C.W., Cowley, T.R., O'Sullivan, J., Grehan, B., Browne, T.C., Kelly, L., Birch, A., Murphy, N., Kelly, A.M., Kerskens, C.M., Lynch, M.A. 2012. The age-related deficit in LTP is associated with changes in perfusion and blood-brain barrier permeability. Neurobiol Aging 33(5), 1005 e23-35. doi:10.1016/j.neurobiolaging.2011.09.035.

Browne, T.C., McQuillan, K., McManus, R.M., O'Reilly, J.A., Mills, K.H., Lynch, M.A. 2013. IFN-γ Production by amyloid β-specific Th1 cells promotes microglial activation and increases plaque

burden in a mouse model of Alzheimer's disease. J Immunol 190(5), 2241-51. doi:10.4049/jimmunol.1200947.

Burgos, J.S., Ramirez, C., Sastre, I., Valdivieso, F. 2006. Effect of apolipoprotein E on the cerebral load of latent herpes simplex virus type 1 DNA. J Virol 80(11), 5383-7. doi:10.1128/JVI.00006-06.

Butovsky, O., Koronyo-Hamaoui, M., Kunis, G., Ophir, E., Landa, G., Cohen, H., Schwartz, M. 2006. Glatiramer acetate fights against Alzheimer's disease by inducing dendritic-like microglia expressing insulin-like growth factor 1. Proc Natl Acad Sci U S A 103(31), 11784-9. doi:10.1073/pnas.0604681103.

Butovsky, O., Kunis, G., Koronyo-Hamaoui, M., Schwartz, M. 2007. Selective ablation of bone marrow-derived dendritic cells increases amyloid plaques in a mouse Alzheimer's disease model. Eur J Neurosci 26(2), 413-6. doi:10.1111/j.1460-9568.2007.05652.x.

Cagnin, A., Brooks, D.J., Kennedy, A.M., Gunn, R.N., Myers, R., Turkheimer, F.E., Jones, T., Banati, R.B. 2001. In-vivo measurement of activated microglia in dementia. Lancet 358(9280), 461-7. doi:10.1016/S0140-6736(01)05625-2.

Dick, A.D., Pell, M., Brew, B.J., Foulcher, E., Sedgwick, J.D. 1997. Direct ex vivo flow cytometric analysis of human microglial cell CD4 expression: examination of central nervous system biopsy specimens from HIV-seropositive patients and patients with other neurological disease. AIDS 11(14), 1699-708.

Downer, E.J., Cowley, T.R., Cox, F., Maher, F.O., Berezin, V., Bock, E., Lynch, M.A. 2009. A synthetic NCAM-derived mimetic peptide, FGL, exerts anti-inflammatory properties via IGF-1 and interferon-gamma modulation. J Neurochem 109(5), 1516-25. doi:JNC6076 [pii]10.1111/j.1471-4159.2009.06076.x.

Dunn, N., Mullee, M., Perry, V.H., Holmes, C. 2005. Association between dementia and infectious disease: evidence from a case-control study. Alzheimer Dis Assoc Disord 19(2), 91-4.

Dunne, A., Ross, P.J., Pospisilova, E., Masin, J., Meaney, A., Sutton, C.E., Iwakura, Y., Tschopp, J., Sebo, P., Mills, K.H. 2010. Inflammasome activation by adenylate cyclase toxin directs Th17 responses and protection against Bordetella pertussis. J Immunol 185(3), 1711-9. doi:10.4049/jimmunol.1000105.

Finkelstein, A., Kunis, G., Seksenyan, A., Ronen, A., Berkutzki, T., Azoulay, D., Koronyo-Hamaoui, M., Schwartz, M. 2011. Abnormal changes in NKT cells, the IGF-1 axis, and liver pathology in an animal model of ALS. PLoS One 6(8), e22374. doi:10.1371/journal.pone.0022374.

Gallagher, J.J., Finnegan, M.E., Grehan, B., Dobson, J., Collingwood, J.F., Lynch, M.A. 2012. Modest Amyloid Deposition is Associated with Iron Dysregulation, Microglial Activation, and Oxidative Stress. J Alzheimers Dis 28(1), 147-61. doi:J76435004P14H16G [pii]10.3233/JAD-2011-110614.

Gallagher, J.J., Minogue, A.M., Lynch, M.A. 2013. Impaired performance of female APP/PS1 mice in the Morris water maze is coupled with increased Aβ accumulation and microglial activation. Neurodegener Dis 11(1), 33-41. doi:10.1159/000337458.

Glass, C.K., Saijo, K., Winner, B., Marchetto, M.C., Gage, F.H. 2010. Mechanisms underlying inflammation in neurodegeneration. Cell 140(6), 918-34. doi:S0092-8674(10)00168-6 [pii10.1016/j.cell.2010.02.016.

Hammond, C.J., Hallock, L.R., Howanski, R.J., Appelt, D.M., Little, C.S., Balin, B.J. 2010. Immunohistological detection of Chlamydia pneumoniae in the Alzheimer's disease brain. BMC Neurosci 11, 121. doi:10.1186/1471-2202-11-121.

Hartwig, M. 1995. Immune ageing and Alzheimer's disease. Neuroreport 6(9), 1274-6.

Holmes, C., Cunningham, C., Zotova, E., Woolford, J., Dean, C., Kerr, S., Culliford, D., Perry, V.H. 2009. Systemic inflammation and disease progression in Alzheimer disease. Neurology 73(10), 768-74. doi:10.1212/WNL.0b013e3181b6bb95.

Holmes, C., El-Okl, M., Williams, A.L., Cunningham, C., Wilcockson, D., Perry, V.H. 2003. Systemic infection, interleukin 1beta, and cognitive decline in Alzheimer's disease. J Neurol Neurosurg Psychiatry 74(6), 788-9.

Honjo, K., van Reekum, R., Verhoeff, N.P. 2009. Alzheimer's disease and infection: do infectious agents contribute to progression of Alzheimer's disease? Alzheimers Dement 5(4), 348-60. doi:10.1016/j.jalz.2008.12.001.

Itzhaki, R.F., Wozniak, M.A., Appelt, D.M., Balin, B.J. 2004. Infiltration of the brain by pathogens causes Alzheimer's disease. Neurobiol Aging 25(5), 619-27. doi:10.1016/j.neurobiolaging.2003.12.021.

Jankowsky, J.L., Fadale, D.J., Anderson, J., Xu, G.M., Gonzales, V., Jenkins, N.A., Copeland, N.G., Lee, M.K., Younkin, L.H., Wagner, S.L., Younkin, S.G., Borchelt, D.R. 2004. Mutant presenilins specifically elevate the levels of the 42 residue beta-amyloid peptide in vivo: evidence for augmentation of a 42-specific gamma secretase. Hum Mol Genet 13(2), 159-70. doi:10.1093/hmg/ddh019ddh019 [pii].

Jimenez, S., Baglietto-Vargas, D., Caballero, C., Moreno-Gonzalez, I., Torres, M., Sanchez-Varo, R., Ruano, D., Vizuete, M., Gutierrez, A., Vitorica, J. 2008. Inflammatory response in the hippocampus of PS1M146L/APP751SL mouse model of Alzheimer's disease: age-dependent switch in the microglial phenotype from alternative to classic. J Neurosci 28(45), 11650-61. doi:28/45/11650 [pii]10.1523/JNEUROSCI.3024-08.2008.

Kitazawa, M., Oddo, S., Yamasaki, T.R., Green, K.N., LaFerla, F.M. 2005. Lipopolysaccharide-induced inflammation exacerbates tau pathology by a cyclin-dependent kinase 5-mediated pathway in a transgenic model of Alzheimer's disease. J Neurosci 25(39), 8843-53. doi:10.1523/JNEUROSCI.2868-05.2005.

Klein, N., Bartlett, J., Rowhani-Rahbar, A., Fireman, B., Baxter, R. 2012. Waning Protection after Fifth Dose of Acellular Pertussis Vaccine in Children. The New England Journal of Medicine (367), 1012-9. doi:10.1056/NEJMoa1200850.

Koenigsknecht-Talboo, J., Landreth, G.E. 2005. Microglial phagocytosis induced by fibrillar beta-amyloid and IgGs are differentially regulated by proinflammatory cytokines. J Neurosci 25(36), 8240-9. doi:25/36/8240 [pii]10.1523/JNEUROSCI.1808-05.2005.

Krstic, D., Madhusudan, A., Doehner, J., Vogel, P., Notter, T., Imhof, C., Manalastas, A., Hilfiker, M., Pfister, S., Schwerdel, C., Riether, C., Meyer, U., Knuesel, I. 2012. Systemic immune challenges trigger and drive Alzheimer-like neuropathology in mice. J Neuroinflammation 9, 151. doi:10.1186/1742-2094-9-151.

Liao, Y.F., Wang, B.J., Cheng, H.T., Kuo, L.H., Wolfe, M.S. 2004. Tumor necrosis factor-alpha, interleukin-1beta, and interferon-gamma stimulate gamma-secretase-mediated cleavage of amyloid precursor protein through a JNK-dependent MAPK pathway. J Biol Chem 279(47), 49523-32. doi:10.1074/jbc.M402034200M402034200 [pii].

Linthicum, D.S., Munoz, J.J., Blaskett, A. 1982. Acute experimental autoimmune encephalomyelitis in mice. I. Adjuvant action of Bordetella pertussis is due to vasoactive amine sensitization and increased vascular permeability of the central nervous system. Cell Immunol 73(2), 299-310.

Little, C.S., Hammond, C.J., MacIntyre, A., Balin, B.J., Appelt, D.M. 2004. Chlamydia pneumoniae induces Alzheimer-like amyloid plaques in brains of BALB/c mice. Neurobiol Aging 25(4), 419-29. doi:10.1016/S0197-4580(03)00127-1.

Liu, Y.J., Guo, D.W., Tian, L., Shang, D.S., Zhao, W.D., Li, B., Fang, W.G., Zhu, L., Chen, Y.H. 2010. Peripheral T cells derived from Alzheimer's disease patients overexpress CXCR2 contributing to its transendothelial migration, which is microglial TNF-alpha-dependent. Neurobiol Aging 31(2), 175-88. doi:S0197-4580(08)00109-7 [pii]10.1016/j.neurobiolaging.2008.03.024.

Lurain, N.S., Hanson, B.A., Martinson, J., Leurgans, S.E., Landay, A.L., Bennett, D.A., Schneider, J.A. 2013. Virological and Immunological Characteristics of Human Cytomegalovirus Infection Associated With Alzheimer Disease. J Infect Dis. doi:10.1093/infdis/jit210.

Man, S.M., Ma, Y.R., Shang, D.S., Zhao, W.D., Li, B., Guo, D.W., Fang, W.G., Zhu, L., Chen, Y.H. 2007. Peripheral T cells overexpress MIP-1alpha to enhance its transendothelial migration in Alzheimer's disease. Neurobiol Aging 28(4), 485-96. doi:S0197-4580(06)00077-7 [pii]10.1016/j.neurobiolaging.2006.02.013.

Mars, L.T., Gautron, A.S., Novak, J., Beaudoin, L., Diana, J., Liblau, R.S., Lehuen, A. 2008. Invariant NKT cells regulate experimental autoimmune encephalomyelitis and infiltrate the central nervous system in a CD1d-independent manner. J Immunol 181(4), 2321-9.

Mattson, M.P. 2004. Pathways towards and away from Alzheimer's disease. Nature 430(7000), 631-9. doi:10.1038/nature02621.

Mayo, L., Quintana, F.J., Weiner, H.L. 2012. The innate immune system in demyelinating disease. Immunol Rev 248(1), 170-87. doi:10.1111/j.1600-065X.2012.01135.x.

McGeer, P.L., Akiyama, H., Itagaki, S., McGeer, E.G. 1989. Immune system response in Alzheimer's disease. The Canadian journal of neurological sciences Le journal canadien des sciences neurologiques 16(4 Suppl), 516-27.

McGeer, P.L., Itagaki, S., Tago, H., McGeer, E.G. 1987. Reactive microglia in patients with senile dementia of the Alzheimer type are positive for the histocompatibility glycoprotein HLA-DR. Neurosci Lett 79(1-2), 195-200.

McGuiness, C.B., Hill, J., Fonseca, E., Hess, G., Hitchcock, W., Krishnarajah, G. 2013. The disease burden of pertussis in adults 50 years old and older in the United States: a retrospective study. BMC Infect Dis 13, 32. doi:10.1186/1471-2334-13-32.

McGuirk, P., Mahon, B.P., Griffin, F., Mills, K.H. 1998. Compartmentalization of T cell responses following respiratory infection with Bordetella pertussis: hyporesponsiveness of lung T cells is associated with modulated expression of the co-stimulatory molecule CD28. Eur J Immunol 28(1), 153-63. doi:10.1002/(SICI)1521-4141(199801)28:01<153::AID-IMMU153>3.0.CO;2-#.

McQuillan, K., Lynch, M.A., Mills, K.H. 2010. Activation of mixed glia by Abeta-specific Th1 and Th17 cells and its regulation by Th2 cells. Brain Behav Immun 24(4), 598-607. doi:S0889-1591(10)00004-8 [pii]10.1016/j.bbi.2010.01.003.

Michaud, J.P., Hallé, M., Lampron, A., Thériault, P., Préfontaine, P., Filali, M., Tribout-Jover, P., Lanteigne, A.M., Jodoin, R., Cluff, C., Brichard, V., Palmantier, R., Pilorget, A., Larocque, D., Rivest, S. 2013. Toll-like receptor 4 stimulation with the detoxified ligand monophosphoryl lipid A improves Alzheimer's disease-related pathology. Proc Natl Acad Sci U S A 110(5), 1941-6. doi:10.1073/pnas.1215165110.

Mills, K.H. 2008. Induction, function and regulation of IL-17-producing T cells. Eur J Immunol 38(10), 2636-49. doi:10.1002/eji.200838535.

Monsonego, A., Zota, V., Karni, A., Krieger, J.I., Bar-Or, A., Bitan, G., Budson, A.E., Sperling, R., Selkoe, D.J., Weiner, H.L. 2003. Increased T cell reactivity to amyloid beta protein in older humans and patients with Alzheimer disease. J Clin Invest 112(3), 415-22. doi:10.1172/JCI18104112/3/415 [pii].

Murooka, T.T., Rahbar, R., Platanias, L.C., Fish, E.N. 2008. CCL5-mediated T-cell chemotaxis involves the initiation of mRNA translation through mTOR/4E-BP1. Blood 111(10), 4892-901. doi:10.1182/blood-2007-11-125039.

Murphy, A.C., Lalor, S.J., Lynch, M.A., Mills, K.H. 2010. Infiltration of Th1 and Th17 cells and activation of microglia in the CNS during the course of experimental autoimmune encephalomyelitis. Brain Behav Immun 24(4), 641-51. doi:S0889-1591(10)00041-3 [pii]10.1016/j.bbi.2010.01.014.

Okello, A., Edison, P., Archer, H.A., Turkheimer, F.E., Kennedy, J., Bullock, R., Walker, Z., Kennedy, A., Fox, N., Rossor, M., Brooks, D.J. 2009. Microglial activation and amyloid deposition in mild cognitive impairment: a PET study. Neurology 72(1), 56-62. doi:72/1/56 [pii]10.1212/01.wnl.0000338622.27876.0d.

Olkhanud, P.B., Mughal, M., Ayukawa, K., Malchinkhuu, E., Bodogai, M., Feldman, N., Rothman, S., Lee, J.H., Chigurupati, S., Okun, E., Nagashima, K., Mattson, M.P., Biragyn, A. 2012. DNA immunization with HBsAg-based particles expressing a B cell epitope of amyloid β-peptide attenuates disease progression and prolongs survival in a mouse model of Alzheimer's disease. Vaccine 30(9), 1650-8. doi:10.1016/j.vaccine.2011.12.136.

Parachikova, A., Agadjanyan, M.G., Cribbs, D.H., Blurton-Jones, M., Perreau, V., Rogers, J., Beach, T.G., Cotman, C.W. 2007. Inflammatory changes parallel the early stages of Alzheimer disease. Neurobiol Aging 28(12), 1821-33. doi:10.1016/j.neurobiolaging.2006.08.014.

Pirttila, T., Mattinen, S., Frey, H. 1992. The decrease of CD8-positive lymphocytes in Alzheimer's disease. J Neurol Sci 107(2), 160-5.

Reale, M., Iarlori, C., Feliciani, C., Gambi, D. 2008. Peripheral chemokine receptors, their ligands, cytokines and Alzheimer's disease. J Alzheimers Dis 14(2), 147-59.

Rogers, J., Luber-Narod, J., Styren, S.D., Civin, W.H. 1988. Expression of immune system-associated antigens by cells of the human central nervous system: relationship to the pathology of Alzheimer's disease. Neurobiol Aging 9(4), 339-49.

Ross, P.J., Sutton, C.E., Higgins, S., Allen, A.C., Walsh, K., Misiak, A., Lavelle, E.C., McLoughlin, R.M., Mills, K.H. 2013. Relative Contribution of Th1 and Th17 Cells in Adaptive Immunity to

Bordetella pertussis: Towards the Rational Design of an Improved Acellular Pertussis Vaccine. PLoS Pathog 9(4), e1003264. doi:10.1371/journal.ppat.1003264.

Saresella, M., Calabrese, E., Marventano, I., Piancone, F., Gatti, A., Alberoni, M., Nemni, R., Clerici, M. 2011. Increased activity of Th-17 and Th-9 lymphocytes and a skewing of the post-thymic differentiation pathway are seen in Alzheimer's disease. Brain Behav Immun 25(3), 539-47. doi:10.1016/j.bbi.2010.12.004.

Sastre, M., Walter, J., Gentleman, S.M. 2008. Interactions between APP secretases and inflammatory mediators. J Neuroinflammation 5, 25. doi:1742-2094-5-25 [pii]10.1186/1742-2094-5-25.

Schall, T.J., Bacon, K., Camp, R.D., Kaspari, J.W., Goeddel, D.V. 1993. Human macrophage inflammatory protein alpha (MIP-1 alpha) and MIP-1 beta chemokines attract distinct populations of lymphocytes. J Exp Med 177(6), 1821-6.

Schenk, D., Barbour, R., Dunn, W., Gordon, G., Grajeda, H., Guido, T., Hu, K., Huang, J., Johnson-Wood, K., Khan, K., Kholodenko, D., Lee, M., Liao, Z., Lieberburg, I., Motter, R., Mutter, L., Soriano, F., Shopp, G., Vasquez, N., Vandevert, C., Walker, S., Wogulis, M., Yednock, T., Games, D., Seubert, P. 1999. Immunization with amyloid-beta attenuates Alzheimer-disease-like pathology in the PDAPP mouse. Nature 400(6740), 173-7. doi:10.1038/22124.

Sedgwick, J.D., Schwender, S., Imrich, H., Dörries, R., Butcher, G.W., ter Meulen, V. 1991. Isolation and direct characterization of resident microglial cells from the normal and inflamed central nervous system. Proc Natl Acad Sci U S A 88(16), 7438-42.

Sheng, J.G., Bora, S.H., Xu, G., Borchelt, D.R., Price, D.L., Koliatsos, V.E. 2003. Lipopolysaccharide-induced-neuroinflammation increases intracellular accumulation of amyloid precursor protein and amyloid beta peptide in APPswe transgenic mice. Neurobiol Dis 14(1), 133-45.

Simard, A.R., Soulet, D., Gowing, G., Julien, J.P., Rivest, S. 2006. Bone marrow-derived microglia play a critical role in restricting senile plaque formation in Alzheimer's disease. Neuron 49(4), 489-502. doi:10.1016/j.neuron.2006.01.022.

Stahl, T., Reimers, C., Johne, R., Schliebs, R., Seeger, J. 2006. Viral-induced inflammation is accompanied by beta-amyloid plaque reduction in brains of amyloid precursor protein

transgenic Tg2576 mice. Eur J Neurosci 24(7), 1923-34. doi:10.1111/j.1460-9568.2006.05069.x.

Strandberg, T.E., Pitkala, K.H., Linnavuori, K., Tilvis, R.S. 2004. Cognitive impairment and infectious burden in the elderly. Arch Gerontol Geriatr Suppl (9), 419-23. doi:10.1016/j.archger.2004.04.053.

Streit, W.J., Conde, J.R., Harrison, J.K. 2001. Chemokines and Alzheimer's disease. Neurobiol Aging 22(6), 909-13.

Sy, M., Kitazawa, M., Medeiros, R., Whitman, L., Cheng, D., Lane, T.E., Laferla, F.M. 2011. Inflammation induced by infection potentiates tau pathological features in transgenic mice. Am J Pathol 178(6), 2811-22. doi:10.1016/j.ajpath.2011.02.012.

Tilvis, R.S., Kähönen-Väre, M.H., Jolkkonen, J., Valvanne, J., Pitkala, K.H., Strandberg, T.E. 2004. Predictors of cognitive decline and mortality of aged people over a 10-year period. J Gerontol A Biol Sci Med Sci 59(3), 268-74.

Togo, T., Akiyama, H., Iseki, E., Kondo, H., Ikeda, K., Kato, M., Oda, T., Tsuchiya, K., Kosaka, K. 2002. Occurrence of T cells in the brain of Alzheimer's disease and other neurological diseases. J Neuroimmunol 124(1-2), 83-92. doi:S0165572801004969 [pii].

Town, T., Laouar, Y., Pittenger, C., Mori, T., Szekely, C.A., Tan, J., Duman, R.S., Flavell, R.A. 2008. Blocking TGF-beta-Smad2/3 innate immune signaling mitigates Alzheimer-like pathology. Nat Med 14(6), 681-7. doi:10.1038/nm1781.

Town, T., Tan, J., Flavell, R.A., Mullan, M. 2005. T-cells in Alzheimer's disease. Neuromolecular Med 7(3), 255-64. doi:NMM:7:3:255 [pii]10.1385/NMM:7:3:255.

Townsend, K.P., Town, T., Mori, T., Lue, L.F., Shytle, D., Sanberg, P.R., Morgan, D., Fernandez, F., Flavell, R.A., Tan, J. 2005. CD40 signaling regulates innate and adaptive activation of microglia in response to amyloid beta-peptide. Eur J Immunol 35(3), 901-10. doi:10.1002/eji.200425585.

Tripathy, D., Thirumangalakudi, L., Grammas, P. 2007. Expression of macrophage inflammatory protein 1-alpha is elevated in Alzheimer's vessels and is regulated by oxidative stress. J Alzheimers Dis 11(4), 447-55.

Tripathy, D., Thirumangalakudi, L., Grammas, P. 2010. RANTES upregulation in the Alzheimer's disease brain: a possible neuroprotective role. Neurobiol Aging 31(1), 8-16. doi:10.1016/j.neurobiolaging.2008.03.009.

Tyas, S.L., Manfreda, J., Strain, L.A., Montgomery, P.R. 2001. Risk factors for Alzheimer's disease: a population-based, longitudinal study in Manitoba, Canada. Int J Epidemiol 30(3), 590-7.

Verreault, R., Laurin, D., Lindsay, J., De Serres, G. 2001. Past exposure to vaccines and subsequent risk of Alzheimer's disease. CMAJ 165(11), 1495-8.

Weiner, H.L., Frenkel, D. 2006. Immunology and immunotherapy of Alzheimer's disease. Nat Rev Immunol 6(5), 404-16. doi:nri1843 [pii]10.1038/nri1843.

Weston, W.M., Friedland, L.R., Wu, X., Howe, B. 2012. Vaccination of adults 65 years of age and older with tetanus toxoid, reduced diphtheria toxoid and acellular pertussis vaccine (Boostrix(®)): results of two randomized trials. Vaccine 30(9), 1721-8. doi:10.1016/j.vaccine.2011.12.055.

Wilcock, D.M., Zhao, Q., Morgan, D., Gordon, M.N., Everhart, A., Wilson, J.G., Lee, J.E., Colton, C.A. 2011. Diverse inflammatory responses in transgenic mouse models of Alzheimer's disease and the effect of immunotherapy on these responses. ASN Neuro 3(5), 249-58. doi:10.1042/AN20110018.

Williams, M. 2009. Progress in Alzheimer's disease drug discovery: an update. Curr Opin Investig Drugs 10(1), 23-34.

Wozniak, M.A., Shipley, S.J., Combrinck, M., Wilcock, G.K., Itzhaki, R.F. 2005. Productive herpes simplex virus in brain of elderly normal subjects and Alzheimer's disease patients. Journal of medical virology 75(2), 300-6. doi:10.1002/jmv.20271.

Xia, M.Q., Bacskai, B.J., Knowles, R.B., Qin, S.X., Hyman, B.T. 2000. Expression of the chemokine receptor CXCR3 on neurons and the elevated expression of its ligand IP-10 in reactive astrocytes: in vitro ERK1/2 activation and role in Alzheimer's disease. J Neuroimmunol 108(1-2), 227-35. doi:S016557280000285X [pii].

Yamamoto, M., Kiyota, T., Horiba, M., Buescher, J.L., Walsh, S.M., Gendelman, H.E., Ikezu, T. 2007. Interferon-gamma and tumor necrosis factor-alpha regulate amyloid-beta plaque deposition and

beta-secretase expression in Swedish mutant APP transgenic mice. Am J Pathol 170(2), 680-92. doi:10.2353/ajpath.2007.060378.

FIGURE LEGENDS

FIGURE 1. Infection induces T cell infiltration in the brain of older APP/PS1 mice.

Mice were infected with *B. pertussis* and culled 56 days postinfection. Mononuclear cells were isolated from the brains of WT and APP/PS1 mice, stained with LIVE/DEAD®, and surface stained for CD45, CD3, CD4 and CD8. Flow cytometric analysis was performed. Results are mean absolute number of the indicated cells in the brain and the diagrams are sample FACS plots of (A) $CD3^+CD45^+$ T cells, (B) $CD4^+CD3^+CD45^+$ T cells and (C) $CD8^+CD3^+CD45^+$T cells, where numbers in FACS plot are percentage of cells positive for the indicated marker. (A) $CD3^+CD45^+$ T cells; Age x genotype x infection interaction $^*p < 0.05$, $F_{(1,43)}=4.22$; 3-way ANOVA. (B) $CD4^+CD3^+CD45^+$ T cells; Infection effect $^{***}p < 0.0001$, $F_{(1,41)}=16.68$; 3-way ANOVA. (C) $CD8^+CD3^+CD45^+$; Age x genotype interaction $^{**}p < 0.01$, $F_{(1,42)}=8.56$ and infection effect $^{**}p < 0.01$, $F_{(1,42)}=9.91$; 3-way ANOVA. $^*p < 0.05$, $^{**}p < 0.01$ in comparison to relevant genotype control; $^{+}p < 0.05$, $^{++}p < 0.01$ in comparison to relevant age control; $^{\#}p < 0.05$, $^{\#\#}p < 0.01$ in comparison to relevant infection control; Newman-Keuls post hoc. Data represent means ± SEM from 3 infection experiments, n=6-9. Abbreviations: Con, Control; *B.P., B. Pertussis*; FSC, Forward Scatter.

FIGURE 2. Respiratory infection induces $IFN\gamma^+$ and $IL\text{-}17^+$ T cell infiltration in the brain of APP/PS1 mice.

$CD4^+$ and $CD8^+$ T cells were intracellularly stained for IFNγ and IL-17 and assessed by flow cytometry. Results are mean absolute number of the indicated cells in the brain. (A) $IFN\gamma^+CD4^+$; Infection effect $^*p < 0.05$, $F_{(1,41)}=5.42$; 3-way ANOVA. (B) $IL\text{-}17^+CD4^+$; Genotype x infection interaction $^*p < 0.05$, $F_{(1,42)}=4.58$; 3-way ANOVA. (C) $IFN\gamma^+IL\text{-}17^+CD4^+$; Infection effect $^{***}p < 0.0001$, $F_{(1,42)}=38.55$; 3-way ANOVA. (E) $IFN\gamma^+CD8^+$; Age x genotype interaction $^*p < 0.05$, $F_{(1,42)}=6.66$; 3-way ANOVA. (F) $IL\text{-}17^+CD8^+$; Genotype x infection interaction $^*p < 0.05$, $F_{(1,42)}=5.46$; 3-way ANOVA. (G) $IFN\gamma^+IL\text{-}17^+CD8^+$; Age x genotype x infection interaction $^*p < 0.05$, $F_{(1,43)}=4.32$; 3-way ANOVA. $^{**}p < 0.01$ in comparison to relevant genotype control; $^{+}p < 0.05$, $^{++}p < 0.01$ in comparison to relevant age control; $^{\#}p < 0.05$, $^{\#\#}p < 0.01$ in comparison to relevant infection control; Newman-Keuls post hoc. (D) Sample

FACS plots of IFNγ^{+} and IL-17^{+} CD4^{+} T cells. (H) Sample FACS plots of IFNγ^{+} and IL-17^{+} CD8^{+} T cells, numbers in FACS plot are percentage of cells positive for the indicated cytokine. Data represent means ± SEM from 3 infection experiments, n=6-9. Abbreviations: Con, Control; *B.P., B. Pertussis*.

FIGURE 3. Infection increases infiltration of IFNγ^{+} and IL-17^{+} NKT cells.

Mononuclear cells were prepared from the brain, stained with LIVE/DEAD®, and surface stained for CD45, NK1.1 and CD3. Cells were intracellularly stained for IFNγ and IL-17, and assessed by FACS. Results are the mean absolute number of the indicated cells in the brain. (A) NK1.1^{+}CD45^{+}CD3^{+} NKT cells; Age x genotype interaction ***$p < 0.001$, $F_{(1,44)}=12.96$; 3-way ANOVA. (B) IFNγ^{+} NKT cells; Age x genotype interaction *$p < 0.05$, $F_{(1,40)}=4.56$; 3-way ANOVA. (C) IL-17^{+} NKT cells; Age x genotype x infection interaction *$p < 0.05$, $F_{(1,43)}=6.38$; 3-way ANOVA. **$p < 0.01$ in comparison to relevant genotype control; $^{+}p < 0.05$, $^{++}p < 0.01$ in comparison to relevant age control; $^{\#}p < 0.05$, $^{\#\#}p < 0.01$ in comparison to relevant infection control; Newman-Keuls post hoc. (D) Sample FACS plots of NK1.1^{+} CD45^{+}CD3^{+} T cells. (E) Sample FACS plots of IFNγ^{+} and IL-17^{+} NKT cells, where the numbers in FACS plot are percentage of cells positive for the indicated marker. Data represent means ± SEM from 3 infection experiments, n=6-9. Abbreviations: Con, Control; *B.P., B. Pertussis*.

FIGURE 4. The increased chemokine expression in older APP/PS1 is exacerbated by infection.

RNA was extracted from snap frozen cortical tissue 56 days postinfection. (A) CCL3, (B) CXCL10, and (C) CCL5 expression was assessed and values are expressed as relative quantities (RQ) normalized to the endogenous control gene, 18S, and relative to the averaged young WT uninfected control group. (A) Age x genotype x infection interaction **$p < 0.01$, $F_{(1,40)}=7.48$; 3-way ANOVA. (B) Age x genotype interaction ***$p < 0.0001$, $F_{(1,41)}=20.13$; 3-way ANOVA. (C) Age x genotype interaction **$p < 0.01$, $F_{(1,41)}=9.18$ and infection effect *$p < 0.05$, $F_{(1,41)}=5.67$; 3-way ANOVA. *$p < 0.05$, **$p < 0.01$ in comparison to relevant genotype control; $^{+}p < 0.05$, $^{++}p < 0.01$ in comparison to relevant age control; $^{\#\#}p < 0.01$ in comparison to relevant infection control; Newman-Keuls post hoc. Data represent means ± SEM from 3 infection experiments, n=6-9. Abbreviations: Con, Control; *B.P., B. Pertussis*.

FIGURE 5. CD11b and GFAP expression is enhanced in older infected APP/PS1 mice.

RNA was extracted from snap-frozen cortical tissue and assessed for (A) CD11b and (B) GFAP expression. Values are expressed as relative quantities (RQ) normalized to the endogenous control gene, 18S, and relative to the averaged young WT uninfected control group. (A) Age x genotype x infection interaction *$p < 0.05$, $F_{(1,43)}=4.09$; 3-way ANOVA. (B) Age x genotype x infection interaction *$p < 0.05$, $F_{(1,42)}=4.26$; 3-way ANOVA. **$p < 0.01$ in comparison to relevant genotype control; $^{++}p < 0.01$ in comparison to relevant age control; $^{\#}p < 0.05$, $^{\#\#}p < 0.01$ in comparison to relevant infection control; Newman-Keuls post hoc. Data represent means ± SEM from 3 infection experiments, n=6-9. Abbreviations: Con, Control; *B.P., B. Pertussis*.

FIGURE 6. Increased microglial activation in APP/PS1 mice.

Mononuclear cells were isolated from the brains of WT and APP/PS1 mice, stained with propidium iodide (PI), and surface stained for CD45, CD11b, CD80 and CD68 and assessed by flow cytometry. Results are mean absolute number of the indicated cells in the brain. (A) $CD11b^{+}CD45^{low}CD80^{+}$; Genotype effect **$p < 0.01$, $F_{(1,42)}=9.69$; 3-way ANOVA, and sample FACS plots of $CD11b^{+}CD45^{low}CD80^{+}$ cells. (B) $CD11b^{+}CD45^{low}CD68^{+}$; Age x genotype x infection interaction *$p < 0.05$, $F_{(1,43)}=5.53$; 3-way ANOVA and sample FACS plots of $CD11b^{+}CD45^{low}CD68^{+}$ cells. Numbers in FACS plot are percentage of cells positive for the indicated marker. *$p < 0.05$, **$p < 0.01$ in comparison to relevant genotype control; $^{++}p < 0.01$ in comparison to relevant age control; $^{\#\#}p < 0.01$ in comparison to relevant infection control; Newman-Keuls post hoc. Data represent means ± SEM from 3 infection experiments, n=6-9. Abbreviations: Con, Control; *B.P., B. Pertussis*.

FIGURE 7. The increased macrophage activation in APP/PS1 is exacerbated by exposure to infection.

Mononuclear cells prepared from WT and APP/PS1 mice were stained with PI, surface stained for CD45, CD11b, CD80 and CD68, then assessed by flow cytometry. Results are mean absolute number of the indicated cells in the brain. (A) $CD11b^{+}CD45^{high}CD80^{+}$; Age x genotype x infection interaction **$p < 0.01$, $F_{(1,41)}=10.73$; 3-way ANOVA with sample FACS plots of $CD11b^{+}CD45^{high}CD80^{+}$ cells. (B) $CD11b^{+}CD45^{high}CD68^{+}$; Age x genotype interaction ***$p < 0.0001$, $F_{(1,39)}=50.44$ and genotype x infection interaction ***$p < 0.0001$, $F_{(1,39)}=22.62$; 3-way ANOVA and sample FACS plots of

$CD11b^{+}CD45^{high}CD68^{+}$ cells, where numbers in FACS plot are percentage of cells positive for the indicated marker. **p < 0.01 in comparison to relevant genotype control; $^{++}p < 0.01$ in comparison to relevant age control; $^{\#}p < 0.05$, $^{\#\#}p < 0.01$ in comparison to relevant infection control; Newman-Keuls post hoc. Data represent means ± SEM from 3 infection experiments, n=6-9. Abbreviations: Con, Control; *B.P., B. Pertussis*.

FIGURE 8. Cytokine expression increased in older APP/PS1 mice.

RNA was extracted from snap frozen cortical tissue and assessed for (A) TNFα, (B) IL-1β, and (C) IL-6 expression. Values are expressed as relative quantities (RQ) normalized to the endogenous control gene, 18S and relative to the averaged young WT uninfected control group. (A) Age x genotype x infection interaction *p < 0.05, $F_{(1,40)}=4.79$; 3-way ANOVA. (B) Age x genotype interaction ***p < 0.001, $F_{(1,41)}=17.42$; 3-way ANOVA. (C) Age x genotype interaction ***p < 0.001, $F_{(1,42)}=8.56$ and age x infection interaction **p < 0.01, $F_{(1,41)}=11.12$; 3-way ANOVA. *p < 0.05, **p < 0.01 in comparison to relevant genotype control; $^{++}p < 0.01$ in comparison to relevant age control; $^{\#}p < 0.05$ in comparison to relevant infection control; Newman-Keuls post hoc. Data represent means ± SEM from 3 infection experiments, n=6-9. Abbreviations: Con, Control; *B.P., B. Pertussis*.

FIGURE 9. Infection increases Aβ plaque number in older APP/PS1 mice.

Cryostat sections were stained with Congo red to assess Aβ plaques in hippocampus (A) and frontal cortex (C) and the average number of plaques per area of interest per mouse was recorded. (B) Mean number of plaques in the hippocampus; Age x infection interaction *p < 0.05, $F_{(1,23)}=4.87$; 2-way ANOVA. (D) Mean number of plaques in the frontal cortex; Age x infection interaction ***p < 0.001, $F_{(1,22)}=25.5$; 2-way ANOVA. ***p < 0.001 in comparison to relevant age control, $^{+}p < 0.05$, $^{+++}p < 0.001$ in comparison to relevant infection control; Newman-Keuls post hoc. Data represent means ± SEM from 3 infection experiments, n=6-9. Abbreviations: Con, Control; *B.P., B. Pertussis*.

FIGURE 10. Insoluble $A\beta_{40}$ increased 56 days post infection in older APP/PS1 mice.

Mice were infected with *B. pertussis* and culled 56 days post infection. Amyloid levels were determined (Meso Scale Discovery, US) from snap-frozen cortical tissue. The concentrations of detergent-soluble $A\beta_{40}$ (A) and $A\beta_{42}$ (B), insoluble $A\beta_{40}$ (C) and $A\beta_{42}$ (D) were established with reference to the standard curves. (A) Age x genotype interaction ***$p < 0.0001$, $F_{(1,40)}=22.46$; 3-way ANOVA. (B) Age x genotype interaction ***$p < 0.0001$, $F_{(1,41)}=40.32$; 3-way ANOVA. (C) Age x genotype x infection interaction *$p < 0.05$, $F_{(1,43)}=4.99$; 3-way ANOVA. (D) Age x genotype interaction **$p < 0.01$, $F_{(1,42)}=8.09$; 3-way ANOVA. *$p < 0.05$, **$p < 0.01$ in comparison to relevant genotype control; $^{++}p < 0.01$ in comparison to relevant age control, $^{\#\#}p < 0.01$ in comparison to relevant infection control; Newman-Keuls post hoc. Data represent means ± SEM from 3 infection experiments, n=6-9. Abbreviations: Con, Control; *B.P., B. Pertussis*.

Figure 1

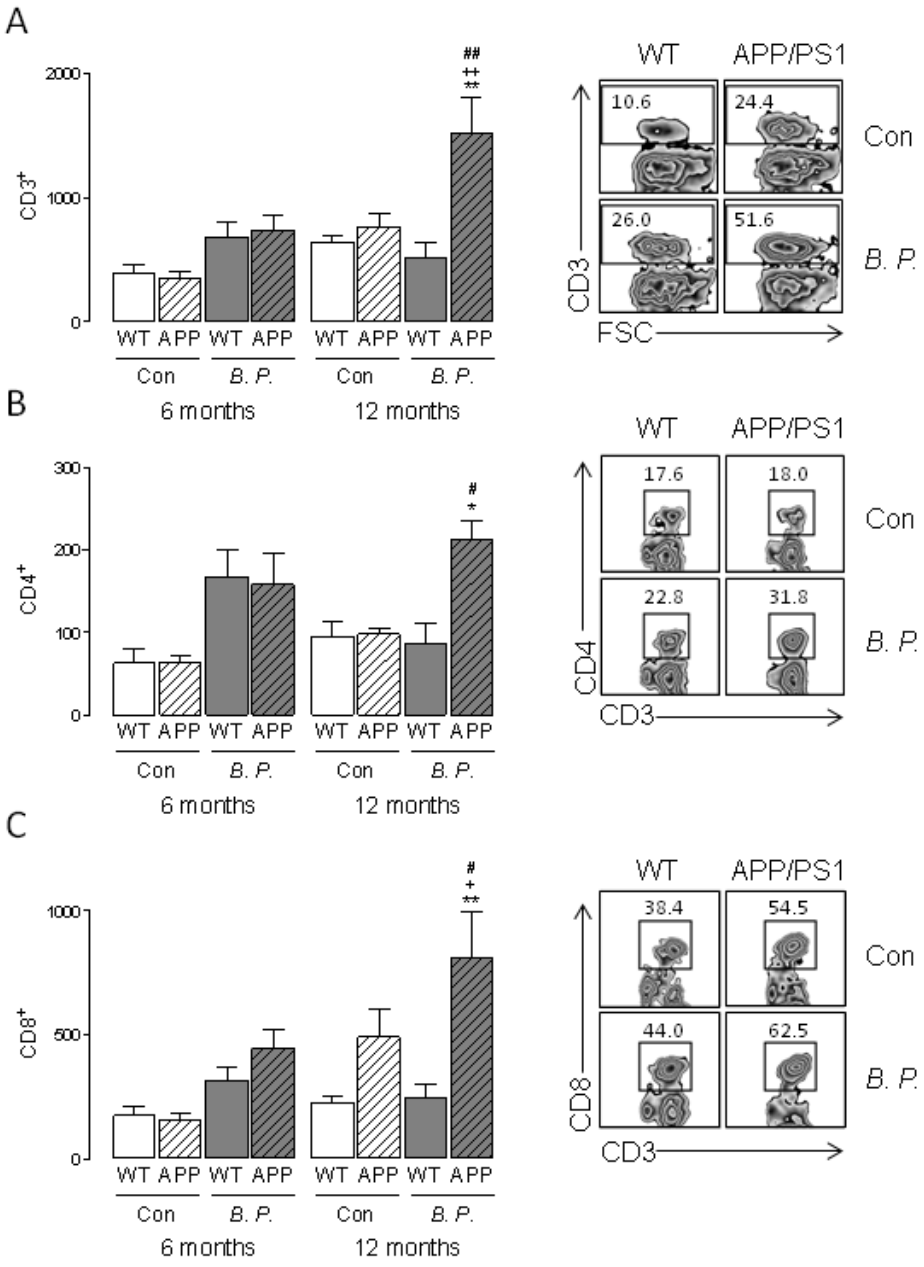
A
CD3+
2000
1000
0
WT APP WT APP WT APP WT APP
Con B. P. Con B. P.
6 months 12 months
##
++
**
WT APP/PS1
10.6
24.4
26.0
51.6
Con
B. P.
CD3
FSC
B
CD4+
300
200
100
0
#
+
*
17.6
18.0
22.8
31.8
CD4
CD3
C
CD8+
1000
500
38.4
54.5
44.0
62.5
CD8

Figure 2

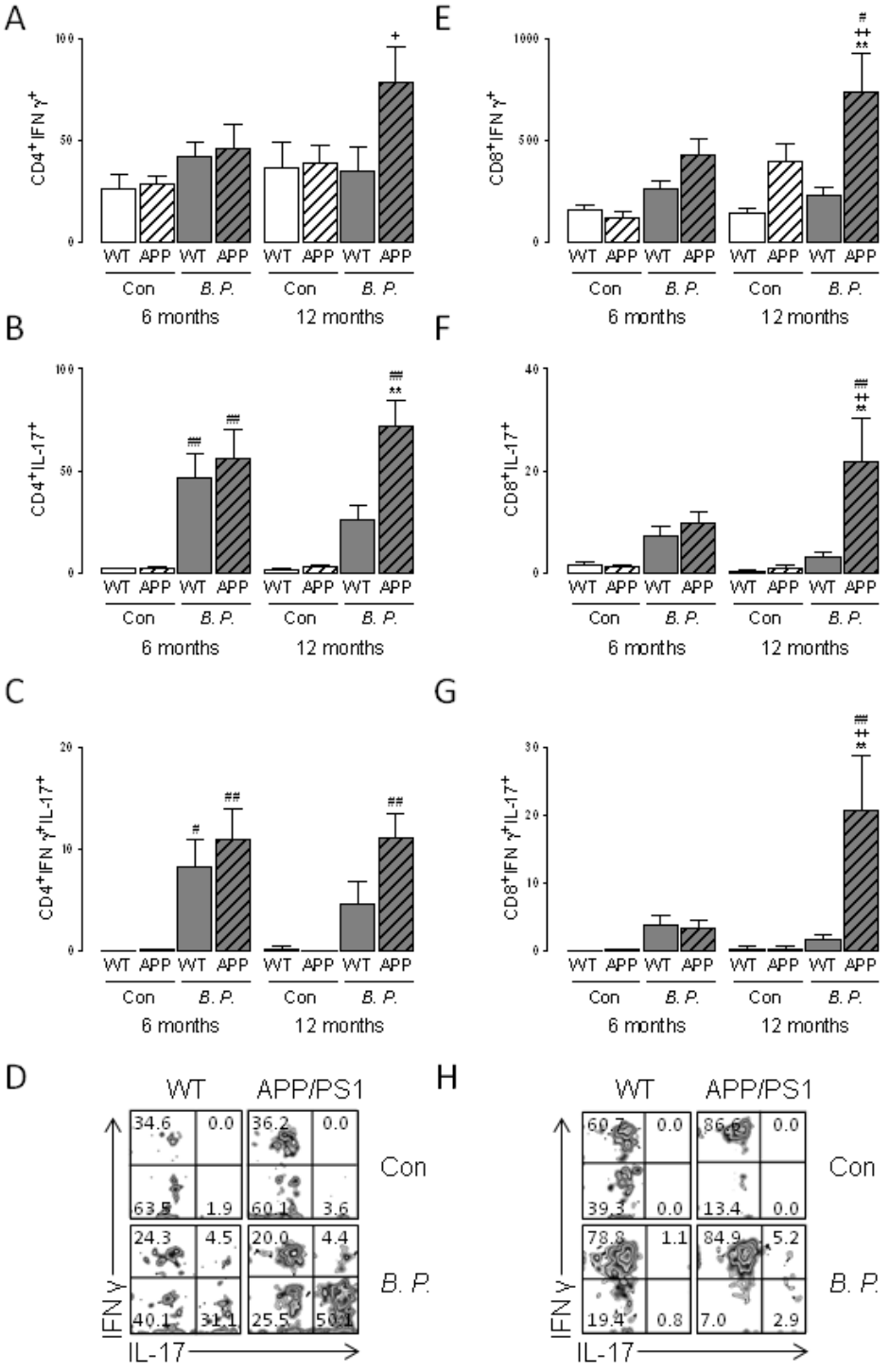
A
E
B
F
C
G
D
H
CD4+IFN γ+
CD8+IFN γ+
CD4+IL-17+
CD8+IL-17+
CD4+IFN γ+IL-17+
CD8+IFN γ+IL-17+
WT APP WT APP WT APP WT APP
Con B. P. Con B. P.
6 months 12 months
WT APP/PS1
Con
B. P.
IFN γ
IL-17
34.6 0.0 36.2 0.0
63.5 1.9 60.1 3.6
24.3 4.5 20.0 4.4
40.1 31.1 25.5 50.1
60.7 0.0 86.6 0.0
39.3 0.0 13.4 0.0
78.8 1.1 84.9 5.2
19.4 0.8 7.0 2.9

Figure 3

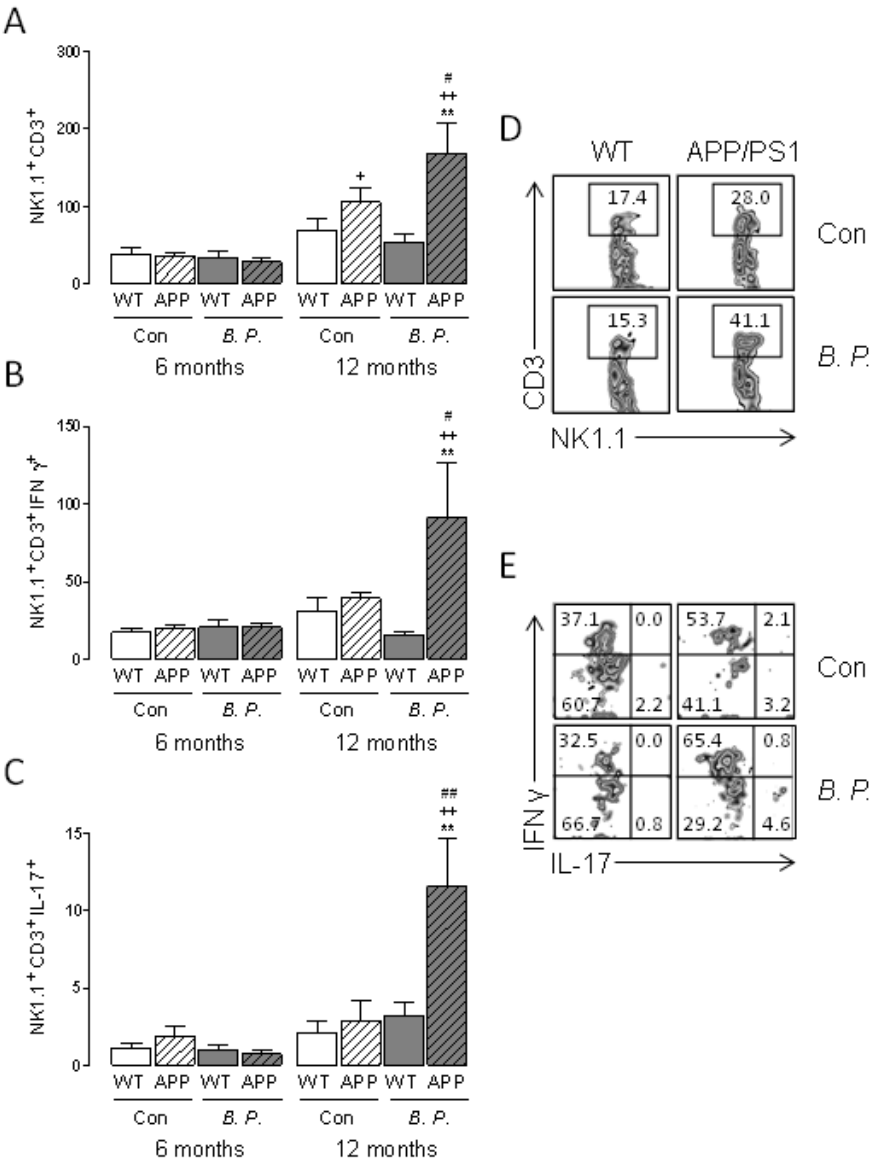
A
NK1.1+CD3+
300
200
100
0
WT APP WT APP WT APP WT APP
Con B. P. Con B. P.
6 months 12 months
B
NK1.1+CD3+IFN γ+
150
100
50
0
C
NK1.1+CD3+IL-17+
15
10
5
0
D
WT APP/PS1
17.4
28.0
15.3
41.1
Con
B. P.
CD3
NK1.1
E
37.1 0.0 53.7 2.1
60.7 2.2 41.1 3.2
32.5 0.0 65.4 0.8
66.7 0.8 29.2 4.6
IFN γ
IL-17

Figure 4

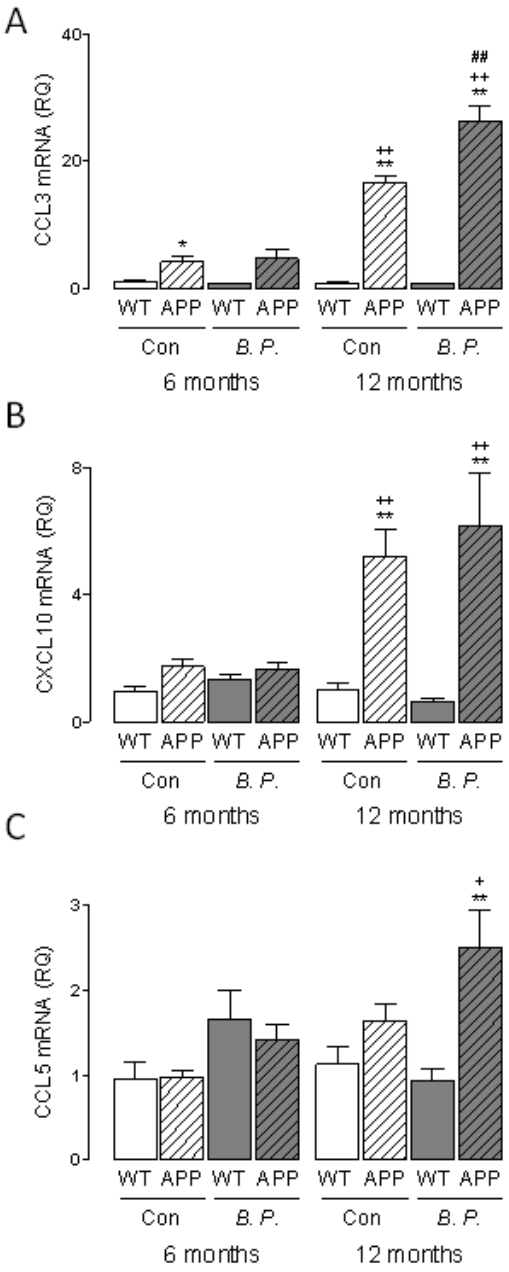
A
CCL3 mRNA (RQ)
40
20
0
*
++
**
##
++
**
WT APP WT APP WT APP WT APP
Con B. P. Con B. P.
6 months 12 months
B
CXCL10 mRNA (RQ)
8
4
0
++
**
++
**
WT APP WT APP WT APP WT APP
Con B. P. Con B. P.
6 months 12 months
C
CCL5 mRNA (RQ)
3
2
1
0
+
**
WT APP WT APP WT APP WT APP
Con B. P. Con B. P.
6 months 12 months

Figure 5

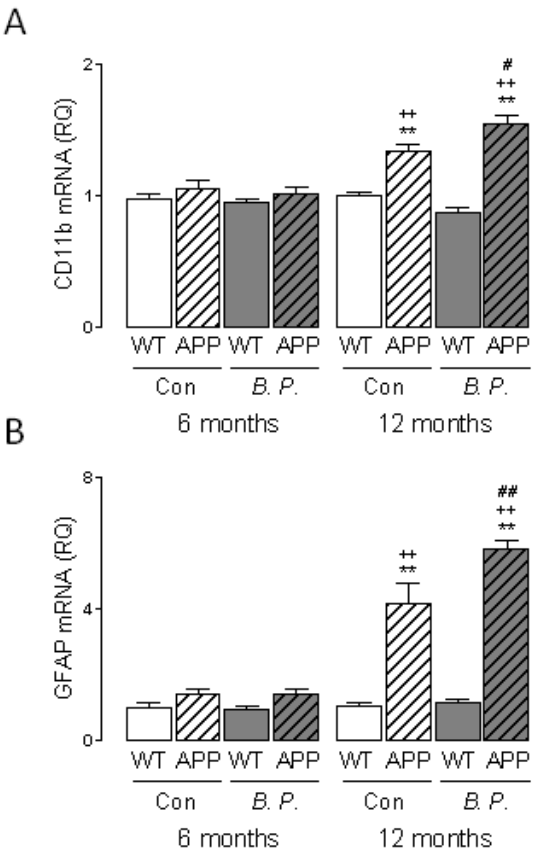
A
CD11b mRNA (RQ)
2
1
0
WT APP WT APP WT APP WT APP
Con B. P. Con B. P.
6 months 12 months
++
**
#
++
**
B
GFAP mRNA (RQ)
8
4
0
WT APP WT APP WT APP WT APP
Con B. P. Con B. P.
6 months 12 months
++
**
##
++
**

Figure 6

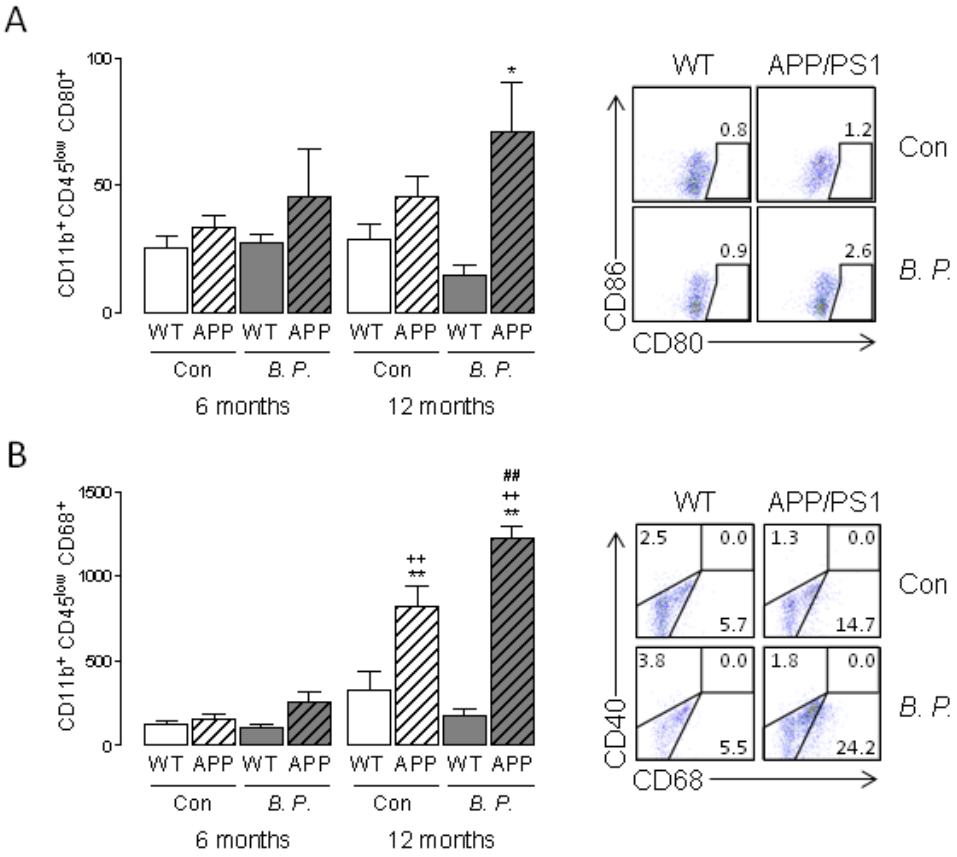
A
CD11b+CD45low CD80+
100
50
0
WT APP WT APP WT APP WT APP
Con B. P. Con B. P.
6 months 12 months
*
WT APP/PS1
0.8
1.2
Con
0.9
2.6
B. P.
CD86
CD80
B
CD11b+ CD45low CD68+
1500
1000
500
0
WT APP WT APP WT APP WT APP
Con B. P. Con B. P.
6 months 12 months
++
**
##
++
**
WT APP/PS1
2.5
0.0
5.7
1.3
0.0
14.7
Con
3.8
0.0
5.5
1.8
0.0
24.2
B. P.
CD40
CD68

Figure 7

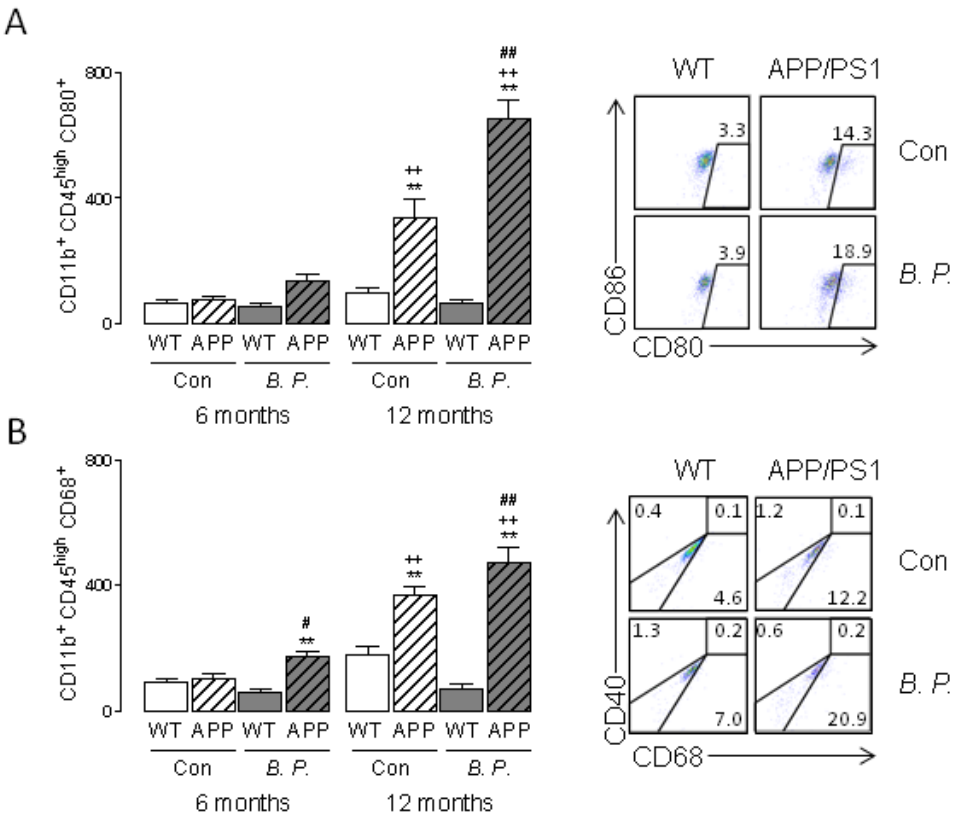
A
CD11b+ CD45high CD80+
800
400
0
WT APP WT APP WT APP WT APP
Con B. P. Con B. P.
6 months
12 months
##
++
**
WT APP/PS1
3.3
14.3
3.9
18.9
Con
B. P.
CD86
CD80
B
CD11b+ CD45high CD68+
#
**
++
**
0.4
0.1
4.6
1.2
0.1
12.2
1.3
0.2
7.0
0.6
0.2
20.9
CD40
CD68

Figure 8

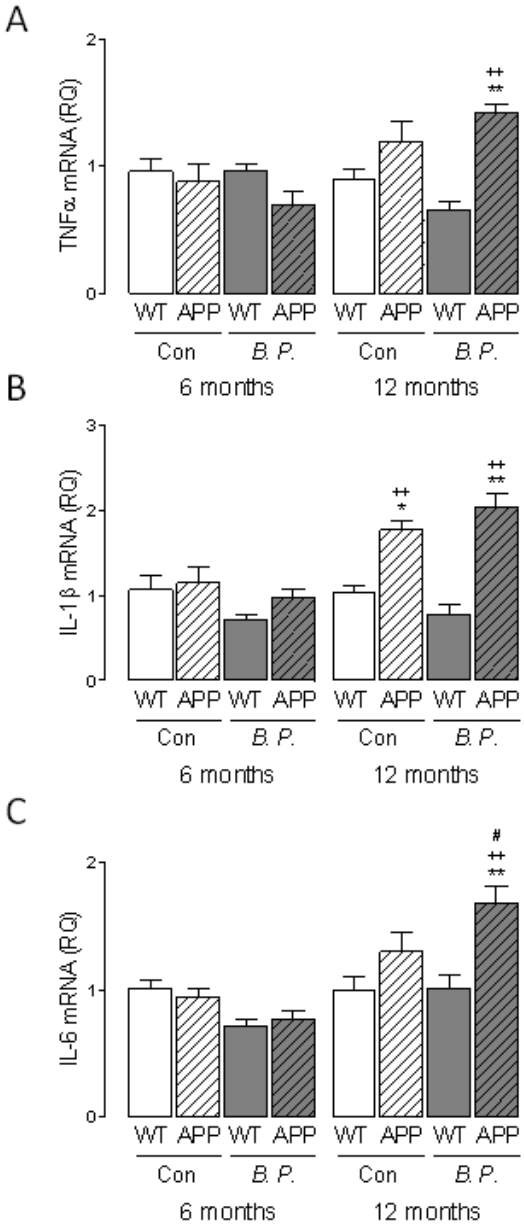
A
TNFα mRNA (RQ)
2
1
0
++
**
WT APP WT APP WT APP WT APP
Con B. P. Con B. P.
6 months 12 months
B
IL-1β mRNA (RQ)
3
2
1
0
++
*
++
**
WT APP WT APP WT APP WT APP
Con B. P. Con B. P.
6 months 12 months
C
IL-6 mRNA (RQ)
2
1
0
#
++
**
WT APP WT APP WT APP WT APP
Con B. P. Con B. P.
6 months 12 months

Figure 9

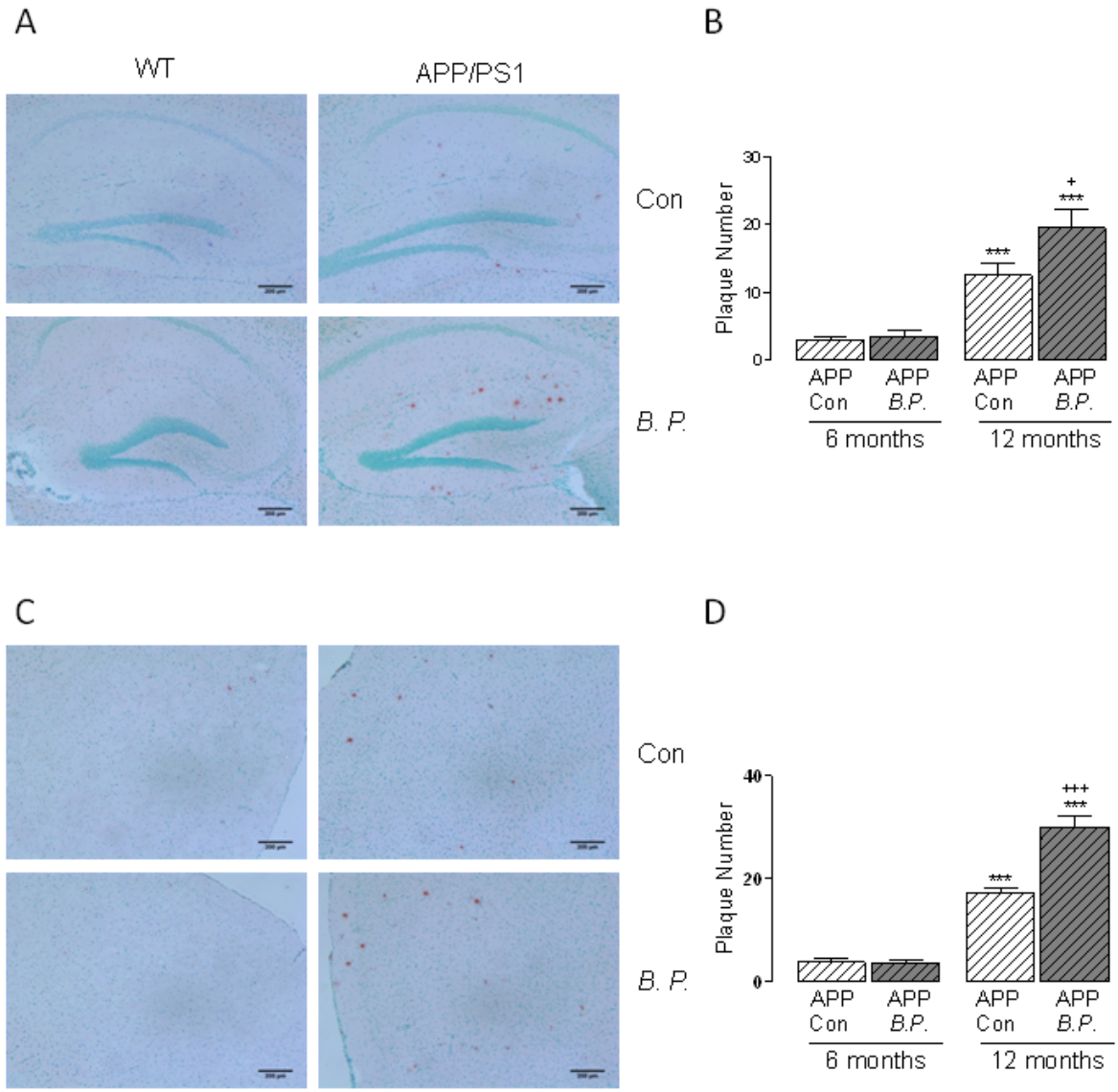
A
WT
APP/PS1
Con
B. P.
B
Plaque Number
30
20
10
0
APP Con
APP B.P.
APP Con
APP B.P.
6 months
12 months
***
+
***
C
D
Con
B. P.
Plaque Number
40
20
0
APP Con
APP B.P.
APP Con
APP B.P.
6 months
12 months
***
+++
***

Figure 10

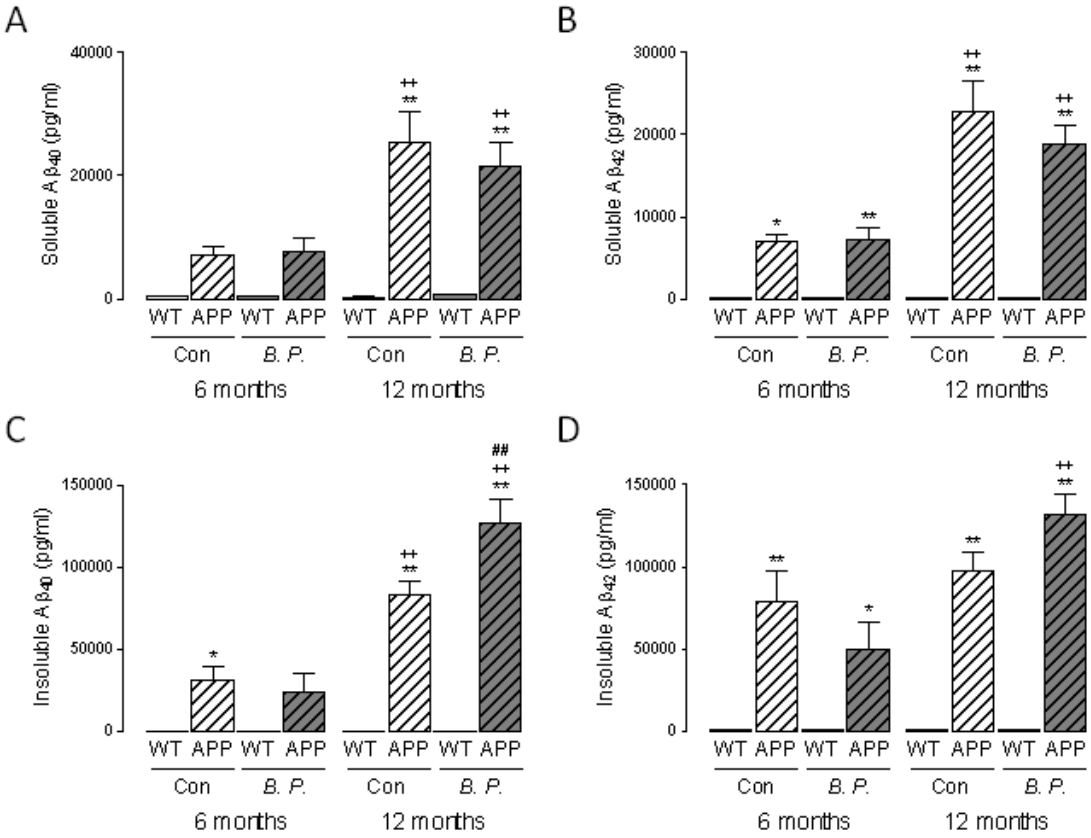
A
B
C
D
Soluble Aβ40 (pg/ml)
Soluble Aβ42 (pg/ml)
Insoluble Aβ40 (pg/ml)
Insoluble Aβ42 (pg/ml)
WT APP WT APP WT APP WT APP
Con B. P. Con B. P.
6 months
12 months